A PARAMETRIC STUDY OF COUNTER FLOW ATOMIZATION

A THESIS

SUBMITTED TO THE FACULTY OF THE

UNIVERSITY OF MINNESOTA DULUTH

BY

COLE ALEXANDER BUCHANAN

IN PARTIAL FUFULLMENT OF THE REQUIREMENTS

FOR THE DEGREE OF

MASTER OF SCIENCE

DR. ALISON HOXIE

MAY 2021

Dedication

To my uncle Mark, you inspired me more than you could have possibly known. I wouldn’t be who I am today without you. Thank you for everything.

"Life is pain. It's how we deal with that pain that defines us."

Mark Paulson 1971 - 2020

Table of Contents

Dedication i

List of Figures v

List of Tables vii

List of Notations viii

Chapter 1 Introduction 1

1.1 Introduction 1

1.2 Goal of this thesis 1

Chapter 2 Theory and Technique 2

2.1 Theory of Atomization 2

2.2 Performance of Atomizers 4

2.2.1 Droplet Size 4

2.2.2 Droplet Uniformity 5

2.2.3 Cost of Twin-Fluid Atomization 6

2.3 Related Twin-Fluid Atomizer Technology 7

2.3.1 Air-assist/Air-blast Atomization 7

2.3.2 Flow-Blurring Atomization 8

2.3.3 Effervescent Atomization 10

Chapter 3 Counterflow Atomization 12

3.1 Counterflow Atomization 12

3.2 Experimental Design 14

3.3 Geometry Characterization 16

3.4 Methodology 16

3.4.1 Air and Water Supply 16

3.4.2 Flow Measurements 17

3.4.3 Droplet Image Analysis 19

Chapter 4 Data Analysis 21

4.1 Results 21

4.1.1 Air vs Water Pressure 21

4.1.2 Air and Water Pressure vs SMD 22

4.1.3 Effect of Flow Rate and GLR on SMD 25

4.1.4 Effect of Doubling Annulus Thickness, t_N on SMD 29

4.1.5 Effect of Doubling Exit Diameter, D_0 on SMD 33

4.2 Discussion 38

4.2.1 Effect of Counterflow Geometry on SMD 38

4.2.2 Proposed Model 42

4.2.3 Effect of Counterflow Geometry on RSF 43

Chapter 5 Conclusion 48

Bibliography 49

Appendix 52

List of Figures

Figure 1. Simplified Pressure Atomizer Cross-Section. 3

Figure 2. Simplified External-Mixing Air-Assist/Air-Blast Atomizer Cross-Section. 4

Figure 3. Simplified Internal-Mixing Air-Assist/Air-Blast Atomizer Cross-Section. 7

Figure 4. Simplified Flow-Blurring Atomizer Cross-Section 9

Figure 5. Simplified Flow-Blurring Exit Region Cross-Section 10

Figure 6. Simplified Effervescent Atomizer Cross-Section 11

Figure 7. Simplified Counterflow Atomizer Cross-Section. 13

Figure 8. Simplified Counterflow Atomizer Exit Region Cross-Section. 13

Figure 9. Tested Counterflow Atomizer Geometries 15

Figure 10. Laser Shadowgraphy System 17

Figure 11. Raw and Processed Droplet Images using ImageJ. 20

Figure 12. CF3 Air vs Water Pressures 22

Figure 13. All Geometries – Measured Inlet Air Pressure vs SMD. 24

Figure 14. All Geometries – Measured Inlet Water Pressure vs SMD 25

Figure 15. CF3 GLR vs Liquid Volumetric Flow Rate 27

Figure 16. CF3 Air and Water Mass Flow Rates vs SMD 28

Figure 17. CF1 vs CF2 – GLR vs Liquid Volumetric Flow Rate 30

Figure 18. CF4 vs CF5 – GLR vs Liquid Volumetric Flow Rate 31

Figure 19. CF1 vs CF2 – Air and Water Mass Flow Rates vs SMD 32

Figure 20. CF4 vs CF5 – Air and Water Mass Flow Rates vs SMD 33

Figure 21. CF1 vs CF4 - GLR vs Liquid Volumetric Flow Rate 35

Figure 22. CF2 vs CF5 - GLR vs Liquid Volumetric Flow Rate 36

Figure 23. CF1 vs CF4 – Air and Water Mass Flow Rates vs SMD 37

Figure 24. CF2 vs CF5 – Air and Water Mass Flow Rates vs SMD 38

Figure 25. All Geometries – Air and Water Mass Flow Rates vs SMD 39

Figure 26. All Geometries – Air and Water Mass Flow Rates vs SMD (Air Mass Flow Rate – SMD plane) 40

Figure 27. All Geometries, SMD/D_0 – Air and Water Mass Flow Rates vs SMD 41

Figure 28. All Geometries, SMD/D_0 – Air and Water Mass Flow Rates vs SMD 42

Figure 29. Modified Counterflow Model 43

Figure 30. SMD vs RSF 44

Figure 31. SMD vs $D_{0.1}$ 45

Figure 32. SMD vs $D_{0.5}$ 46

Figure 33. SMD vs $D_{0.9}$ 47

Figure 34. CF1 Liquid Volumetric Flow Rate vs GLR 52

Figure 35. CF2 Liquid Volumetric Flow Rate vs GLR 53

Figure 36. CF3 Liquid Volumetric Flow Rate vs GLR 54

Figure 37. CF4 Liquid Volumetric Flow Rate vs GLR 55

Figure 38. CF5 Liquid Volumetric Flow Rate vs GLR 56

List of Tables

Table 1. Tested Counterflow Atomizer Geometries. 14

Table 2. Tested Liquid Volumetric Flow Rates 15

Table 3. CF3 SMD at a Water Pressure of 1.13 bar 23

Table 4. CF3 Flow Settings for an SMD of Approximately 17 Microns 24

Table 5. Effects of Doubling Exit Diameter on SMD 34

List of Notations

Abbreviations:

GLR gas-to-liquid mass flow ratio

SMD Sauter mean diameter (d_{32} in equations)

Symbols:

ρ mass density

Nomenclature:

D diameter

d_{32} Sauter mean diameter (abbreviated SMD in text)

MMD mass median diameter ($D_{0.5}$ in equations)

$\dot{m}$ mass flow rate

P absolute pressure

Q volumetric flow rate

t annulus gap thickness

Subscripts:

0 exit orifice

G gas

L liquid

N counterflow annulus

STP standard temperature and pressure

Chapter 1 Introduction

1.1 Introduction

Novel atomizers using counterflow gas injection have shown the potential to produce water sprays comparable to commercial air-assist internal-mixing atomizers at up to 50% energy savings, with even larger savings possible for higher viscosity liquids [22]. Furthermore, counterflow atomization was shown to produce sprays with centerline Sauter mean diameters (SMD or d_{32}) that are weakly sensitive over two magnitudes to liquid viscosity [23]. A preliminary model was posed by Johnson and colleagues [21] relating the observed effects of annulus thickness (t_N), gas molar mass, and gas-to-liquid mass ratio (GLR) on the centerline SMD produced by counterflow atomizers. In their study, the effects of injection gas molar mass were determined that, in contrast to effervescent or co-flow atomizers, gasses with lighter molar masses produce sprays of significantly smaller SMD [21] [27].

1.2 Goal of this thesis

This study investigates the effects of liquid volumetric flow rate, GLR, and counterflow atomizer exit orifice diameter, D_0 and annulus thickness, t_N on the atomizer's performance in terms of the resultant sprays' centerline SMD and relative span factor (RSF). In doing so, a modified model is proposed relating

flow conditions to atomizer performance leading to a further understanding of the physical mechanisms of counterflow atomization.

Chapter 2 Theory and Technique

2.1 Theory of Atomization

Atomization is the process of transforming a jet or column of liquid into a dispersed phase of droplets. This process is important for several industrial processes and has numerous applications of which can be broken into three general categories: Impact-related spray processes, spray structure-related processes, and particle production-related processes. Impact-related spray processes involve utilizing the dispersed liquid phase to coat an object such as in corrosion protections, crop and plant production, and spray cooling/heat treatment of metals. Spray structure-related spray processes take advantage of the distribution of liquid or solids within a gaseous environment in heat exchange processes like air conditioning or reaction processes for combustion applications. Lastly, particle production-related processes rely on the high heat and mass transfer rates obtainable by atomization such as the formation of powdered metals or spray drying of solutions [1] [3] [4].

Single-Fluid atomization, also known as pressure atomization or hydraulic atomization, is one of the most commonly used methods in general application

areas [6]. The liquid is discharged from the atomizer at high velocity relative to the surrounding ambience causing instabilities and breakup [2] [4] [6] . A simplified diagram of a pressure atomizer can be seen in Figure 1. A variety of internal geometries exist ranging from swirlers to converging and diverging exits as well as multi-hole exits.

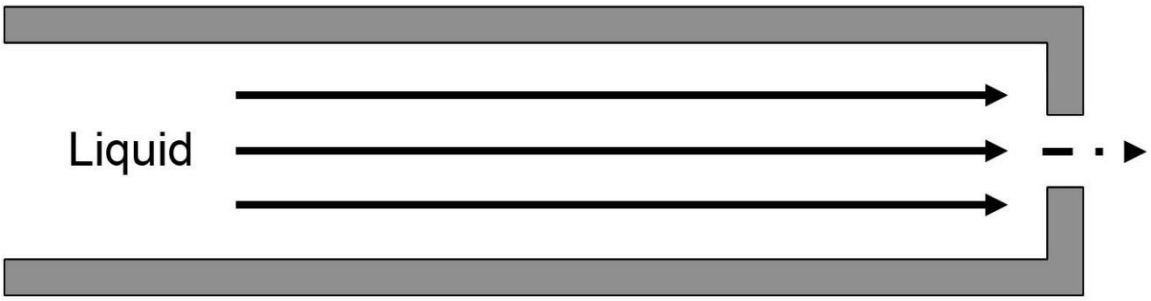

Figure 1. Simplified Pressure Atomizer Cross-Section.

Twin-fluid atomization is a broad category of atomization in which the liquid to be atomized is exposed to a gas either within (internal-mixing type) or outside (external-mixing type) the atomizer geometry. In general, twin-fluid atomization a low velocity liquid is impacted by a high velocity gas which causes instabilities in the liquid causing breakup [2] [4] [6]. A simplified diagram of an external-mixing, air-assist/air-blast atomizer can be seen in Figure 2.

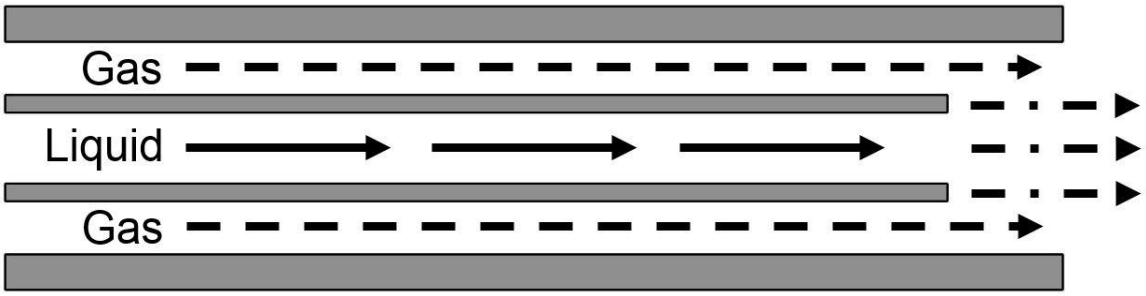

Figure 2. Simplified External-Mixing Air-Assist/Air-Blast Atomizer Cross-Section.

2.2 Performance of Atomizers

2.2.1 Droplet Size

Due to the range of drop sizes present within any given spray, both mean diameters and drop size distributions are necessary when defining the quantitative behavior of the spray [2] [4] [33]. Sauter mean diameter (SMD or d_{32}) is commonly used in mass transfer or reaction applications and represents the diameter of a single droplet with the same total surface area to volume ratio as the observed spray as seen in Equation 1.

$$SMD = d_{32} \stackrel{\text{def}}{=} \frac{\sum d_i^3}{\sum d_i^2} \qquad \text{Eqn. 1}$$

Where d_i^3 is the individual droplet diameter cubed and d_i^2 is the individual droplet diameter squared.

2.2.2 Droplet Uniformity

Relative span factor (RSF) is a nondimensional measure of droplet uniformity. RSF provides a ratio of the ranges of droplet sizes within the spray to the mass median diameter (MMD or $D_{0.5}$) of the spray. In particular, it is defined by the 90th, 50th, and 10th volume-weighted droplet diameter distribution as seen in Equation 2 where $D_{0.9}$ represents the diameter of droplets which 90% of the volume of the spray is smaller than, $D_{0.5}$ represents the diameter of droplets which 50% of the volume of the spray is smaller than, and $D_{0.1}$ represents the diameter of droplets which 10% of the volume of the spray is smaller than.

$$RSF \stackrel{\text{def}}{=} \frac{D_{0.9} - D_{0.1}}{D_{0.5}} \qquad \text{Eqn. 2}$$

As droplet sizes approach uniformity, RSF decreases towards 0. In most cases, the drop size distribution of a spray is as equally important as median diameters. Impact-related spray processes such as painting require narrow drop size distributions as small outlying droplets can decrease transfer efficiency. Additionally, narrow drop size distributions are also advantageous in combustion applications as large outlying drops tend to increase emissions. In contrast, gas turbines require a wide droplet size distribution [4] [27]

2.2.3 Cost of Twin-Fluid Atomization

Twin-fluid atomization generally utilizes high velocity gasses in order to shatter the liquid to be atomized. Gas-to-liquid mass flow ratio (GLR), as seen in Equation 3 serves as a quantitative cost metric, as the energy required to compresses gasses is much greater than that to supply liquids [27]. In general, twin-fluid atomization sees a decrease in SMD for an increase in GLR [17] [20] [33]. This decrease in SMD is generally due to an increase of the kinetic energy of the atomizing gas which impacts the liquid. However, this decrease in SMD with increasing GLR comes with diminishing returns such that one geometry may only provide a narrow distribution of attainable mean diameters. As such, atomizer design, in particular the internal geometry of twin fluid atomizers, plays a large role in the final mean diameters of the spray [33].

$$\beta = GLR \stackrel{\text{def}}{=} \frac{\dot{m}_G}{\dot{m}_L} \qquad \text{Eqn. 3}$$

Where β is the gas to liquid mass flow rate ratio and $\dot{m}_G \text{ and } \dot{m}_L$ are the gas and liquid mass flow rates respectively.

2.3 Related Twin-Fluid Atomizer Technology

2.3.1 Air-assist/Air-blast Atomization

Both air-assist and air-blast atomization are twin-fluid atomization techniques in which a relatively low-velocity liquid stream is impacted by a high-velocity gas causing liquid instabilities due to the kinetic energy of the gas leading to jet breakup [2] [24]. The gas can be injected either within or outside of the nozzle geometry and are appropriately referred to as *internal* or *external* mixing types. A simplified schematic of an axisymmetric air-assist/air-blast atomizer with internal-mixing and a co-flow geometry can be seen in Figure 3. Like pressure-atomizers, a wide variety of internal geometries exist with mixing chambers, flow swirlers, converging and diverging exits, as well as multi-hole exits.

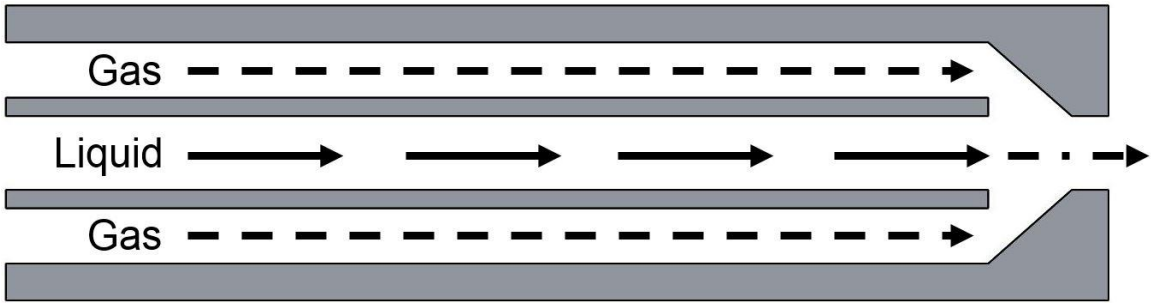

Figure 3. Simplified Internal-Mixing Air-Assist/Air-Blast Atomizer Cross-Section.

The key distinction between air-assist and air-blast atomization is the total amount of pressurized gas and its velocity used to atomize liquids. While an air-assist atomizer has no restriction on pressure or gas velocity, air-blast atomizers

typically are limited as required for combustion applications and, as such, have increased mass flow rate of gas to achieve the necessary drop sizes [2] Additionally, most air-assist and air-blast atomizers are of a prefilming type that spread the liquid into thin sheet prior to it being impacted by the gas as the mean drop size is a function of the liquid film/sheet thickness [2] [24]. For air-blast in particular, Lefebvre and Miller identified that the finest sprays were produced when the liquid sheet had the minimum thickness [2] [26].

For both air-assist and air-blast atomization, empirical correlations of mean droplet sizes generally use exit diameter and GLR as well as the physical properties of the working fluids [2]. in a comparison of air-assist atomizers with radial and axial air swirlers done by Levy et al. it was found that there were no effects on droplet size for air-to-liquid mass ratios ranging from 1 to 4 [25] Furthermore, work by Lefebvre and Miller found that for air-to-liquid mass ratios of 3 to 9 had little effect on the atomization quality [26] [28]

2.3.2 Flow-Blurring Atomization

Flow-blurring atomization utilizes an internal geometry that injects the atomizing gas perpendicularly to the liquid flow, causing a portion of the injected atomizing gas to flow up-stream into the liquid tube and mix turbulently with the liquid [14]. The internal two-phase mixing creates a bubbly mixture and as it exits the

atomizer, the gas phase expands shattering the liquid into droplets [10] [11] [12] [13] [14]. A simplified schematic of a flow-blurring atomizer can be seen in Figure 4.

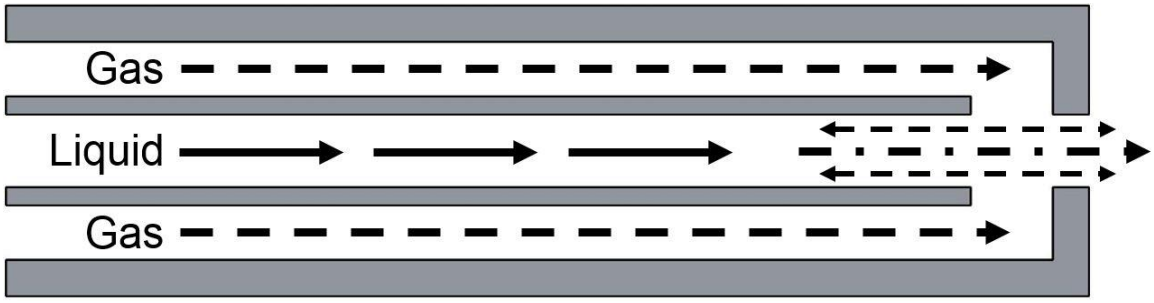

Figure 4. Simplified Flow-Blurring Atomizer Cross-Section.

Flow-blurring atomization occurs when the ratio of gap height to exit diameter ratio is less than or equal to 0.25 ($h/D \leq 0.25$) as seen in Figure 5. [14]. As such, the exit diameter plays a role in the atomization process but no results directly relating exit orifice diameters and mean drop sizes have been reported. GLR values have been tested from less than 1 to well over 100 [10] [11] [12] [13] [14].

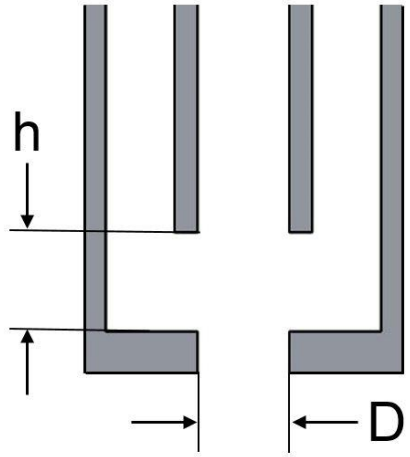

Figure 5. Simplified Flow-Blurring Exit Region Cross-Section

2.3.3 Effervescent Atomization

In contrast to the twin-fluid atomizers mentioned previously, effervescent atomization makes use of a bubbly, two-phase flow that occurs due to a low difference in pressures between the injected atomizing gas and liquid rather than the kinetic energy of the gas itself [2] [4] [18] [20]. It was originally thought that this bubbly mixture pinches the liquid in the exit orifice forming ligaments, as the two-phase mixture exits the nozzle, the gas bubbles rapidly expand due to choking causing the ligaments to subsequently shatter into droplets [2] [4] [18] [20]. However, in a more recent study by Shepard and Garbaly, they found evidence of subcritical flow both above and below theoretically critical conditions that should cause evidence of choking in an effervescent atomizer geometry [16]. A simplified schematic of an effervescent atomizer can be seen in Figure 6.

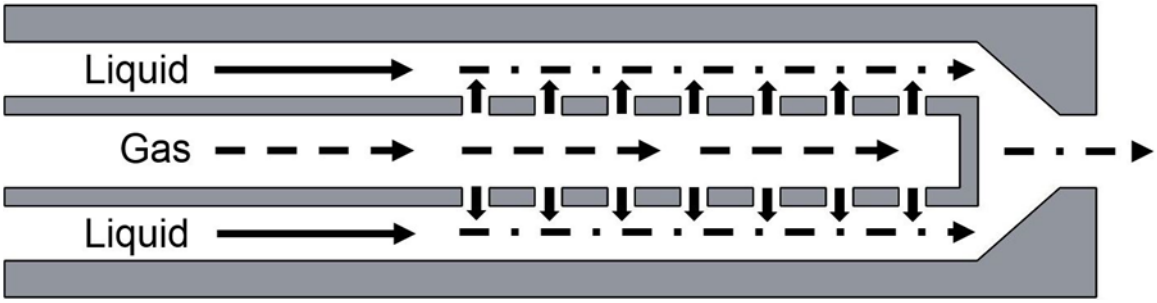

Figure 6. Simplified Effervescent Atomizer Cross-Section with "inside-out" gas injection

Effervescent atomization techniques can vary by either using outside-in gas injection (OIG) or an inside-out gas injection format, also known as outside-in-liquid (OIL) which differ only in where the fluids are injected [17] [20]. In an outside-in format, liquid flows through a central, perforated tube in which gas is bubbled into. In the OIL format, gas is injected into a central perforated tube and bubbles out into the liquid. In a study performed by Mlkvik and Knizat, they compared an effervescent atomizer using both an OIL and OIG format at a constant injection pressure of 0.14 MPa and GLR of 2.5% and 5% with an aqueous maltodextrin solution as the working fluid an OIG and OIL format [17]. It was found that the format plays a significant effect on both the flow regimes observed and consequently the mean drop sizes and distributions.

Effervescent atomization operates at much lower GLR than other twin-fluid atomization types with SMD data having been acquired from GLR ranging from 0.001 by Roesler and Lefebvre to 0.85 by Li et al. [20] [28]. As with other twin-fluid atomization types, spray SMD has been shown to be a nonlinear function of

GLR where SMD decreases rapidly with increasing GLR with diminishing returns around a GLR of 0.03 [4] [18] [20]. Unlike other atomizer types, droplet size appears to be largely independent of final orifice diameter [2] [19] [20].

Chapter 3 Counterflow Atomization

3.1 Counterflow Atomization

Counterflow atomization is a twin-fluid atomization technique similar in geometry to flow-blurring atomization. Though the mechanism not yet fully defined in terms of flow regimes, counterflow atomization is thought to exploit the high turbulent stresses associated with countercurrent flow fields to accomplish complete and efficient internal mixing [27] [30]. Studies have shown counterflow atomization's ability to produce sprays of similar or better quality than that of commercial internal-mixing type air-assist atomizers at half or less than half of the gas supply costs for both water and liquids with viscosities 40 times that of water [22]. Furthermore, the centerline SMD of counterflow atomizers were determined to be greatly affected by injection gas molar mass, with lighter gasses producing sprays with significantly lower SMD in contrast to effervescent or co-flow literature [21] [27]. Most recently counterflow atomization showed the potential to produce sprays with smaller SMDs than a comparable flow-blurring atomizer at the same flow conditions using both water and glycol as test fluids. Additionally, high-fidelity simulations suggested the mechanism responsible for spray

formation is a Kelvin-Helmoltz-type instability of the liquid jet inside the nozzle [23]. A simplified schematic of a counterflow atomizer can be seen in Figure 7.

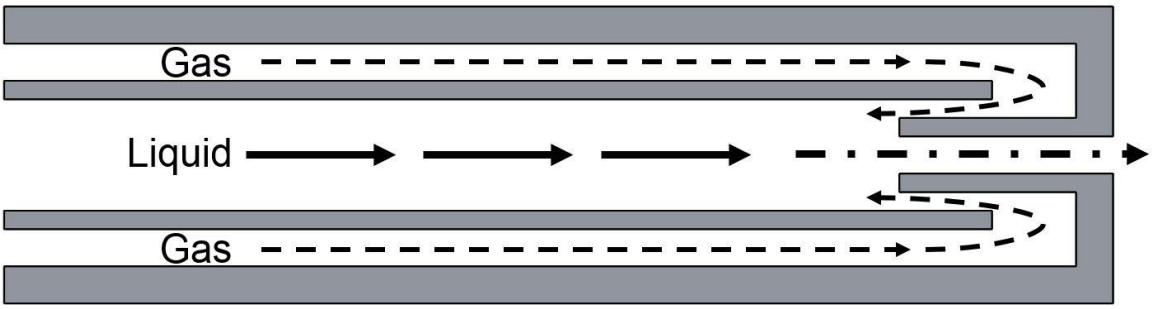

Figure 7. Simplified Counterflow Atomizer Cross-Section.

The internal geometry of counterflow atomization consists of two overlapping tubes. The liquid tube of slightly larger diameter overhangs the central exit tube. Gas is injected through the anulus area of thickness t_N and mixing is instigated in the liquid tube before exiting through the exit orifice D_0 as seen in Figure 8.

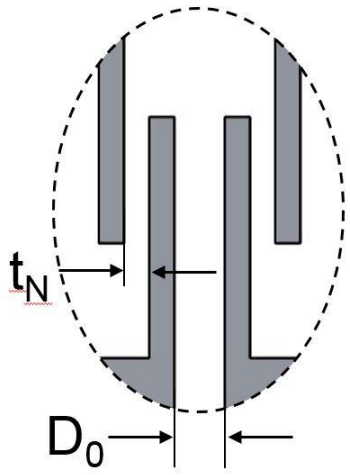

Figure 8. Simplified Counterflow Atomizer Exit Region Cross-Section.

3.2 Experimental Design

This parametric study aims to determine which internal geometry has the greatest effect on the performance of 5 different counterflow atomizer geometries whose dimensions are given in Table 1 and are graphically represented in Figure 9. Where CF1 has an exit diameter of 1.196 millimeters and an annulus thickness of 0.174 millimeters; CF2 has an exit diameter of 1.196 millimeters and an annulus thickness of 0.331 millimeters; CF3 has an exit diameter of 1.830 millimeters and an annulus thickness of 0.274 millimeters; CF4 has an exit diameter of 2.341 millimeters and an annulus thickness of 0.164 millimeters; and CF5 has an exit diameter of 2.341 millimeters and an annulus thickness of 0.353 millimeters. Each geometry was tested at liquid volumetric flow rates of 15.8 (16), 31.5 (32), 63.1 (64), 126.2 (125), 315.5 (315), and 630.9 (630) cubic centimeters per minute as seen in Table 2. At each liquid flow rate, the gas mass flow rate was varied such that the GLR was 0.2, 0.5, 1.0, and 2.0 for each liquid volumetric flow rate setting respectively, leading to a total of 24 possible flow settings comparable for each atomizer.

Table 1. Tested Counterflow Atomizer Geometries.

Atomizer	D_0 (micron, 95%)	t_N (micron, 95%)
CF1	1196 ± 5	174 ± 5
CF2	1196 ± 5	331 ± 5
CF3	1830 ± 3	274 ± 8
CF4	2341 ± 6	164 ± 4
CF5	2341 ± 6	353 ± 6

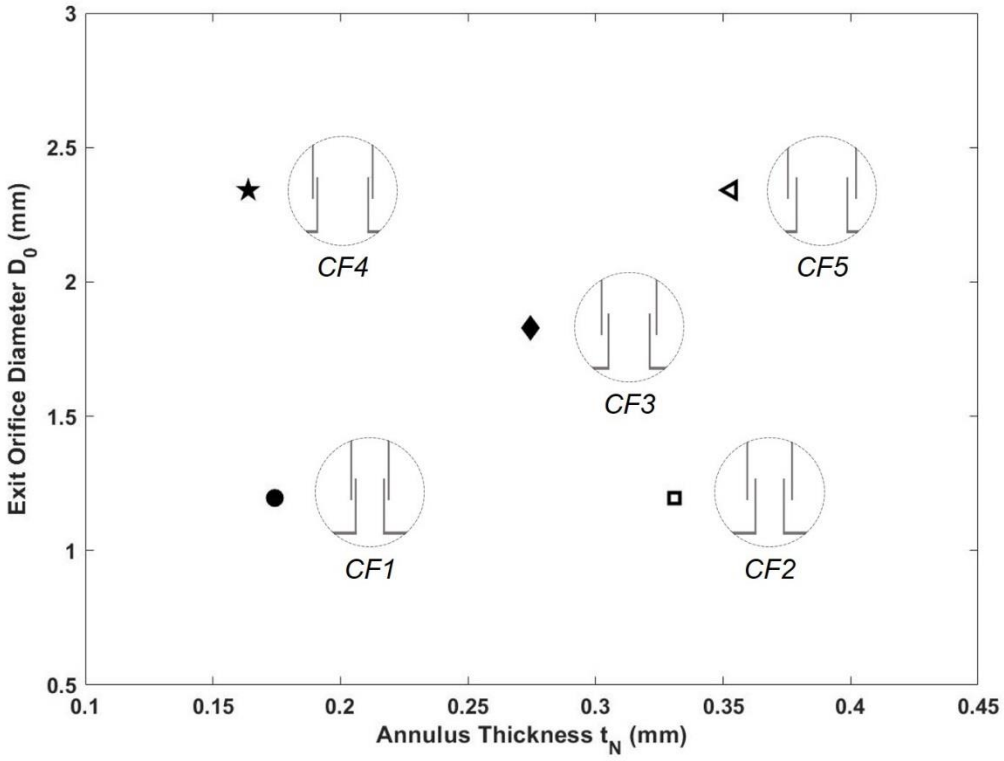

Figure 9. Tested Counterflow Atomizer Geometries. CF1 (filled circles), CF2 (unfilled squares), CF3 (filled diamonds), CF4 (filled stars), CF5 (unfilled left-pointing triangles)

Table 2. Tested Liquid Volumetric Flow Rates

Milliliters Per Minute	Meters cubed per second	US Gallons Per Hour
15.8	2.63E-7	0.25
31.5	5.26E-7	0.5
63.1	1.05E-7	1.0
126.2	2.10E-6	2.0
315.5	5.26E-6	5.0
630.9	1.05E-5	10.0

**All liquid volumetric flow rates tested at 0.2, 0.5, 1.0, and 2.0 GLR respectively.*

3.3 Geometry Characterization

Counterflow atomizer CF1 was chosen as it was the smallest combination of exit orifice diameter and annulus thickness available for testing at the time of this present study. The remainder of the geometries chosen for this study aim to reveal the effects of approximately doubling the exit orifice diameter at an approximately constant annulus gap thickness; and approximately doubling the annular gap thickness at a constant exit orifice diameter.

3.4 Methodology

3.4.1 Air and Water Supply

The experimental setup used in this study is shown in Figure 10. Water was supplied via a 2.8 gallon Binks 83C Series pressure tank (Carlisle Fluid Technologies, Scottsdale, AZ) pressurized with shop air with a max output pressure of approximately 551 kilopascals (80 psig). Air was supplied to both the nozzle and pressure tank by a Quincy QR-25 reciprocating compressor fitted with a 50 gallon reservoir (Quincy Compressor, Bay Minette, AL)

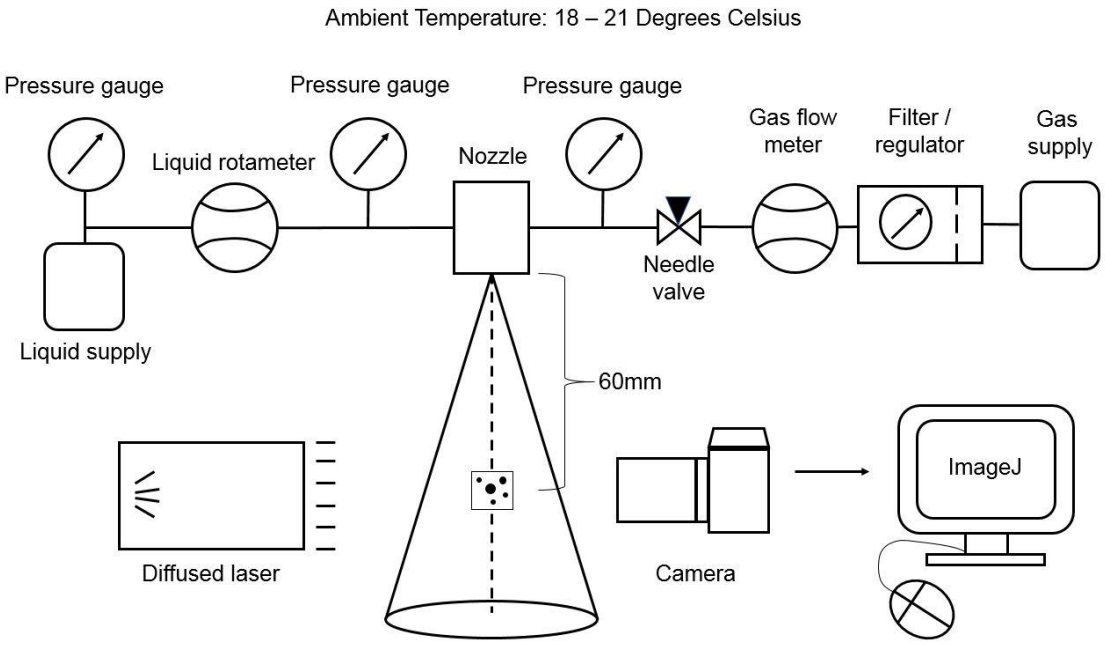

Figure 10. Laser Shadowgraphy System

3.4.2 Flow Measurements

Water flow rates were achieved by supplying sufficient air pressure for a given flow rate to the Binks pressure tank. The flow rate was then fine-tuned and measured with Cole-Parmer variable-area, acrylic rotameters with ±3% full-scale accuracy. Room temperature water varied by less than 5 degrees Celsius and as such the water mass density was estimated to be 998 ± 2 kg/m^3. Air volumetric flow rate at Standard Temperature and Pressure (STP) was measured with a 1-500 SLPM Cole-Parmer digital gas flowmeter (laminar flow element type) with a ±0.8% reading accuracy and ±0.2% of full-scale accuracy. The uncertainty of air

gas mass density at STP was estimated to be 1%. GLR was determined via Equation 4,

$$\beta = GLR \stackrel{\text{def}}{=} \frac{\dot{m}_G}{\dot{m}_L} = \frac{Q_{G,STP}\,\rho_{G,STP}}{Q_L\,\rho_L} \qquad \text{Eqn. 4}$$

Where Q_G and Q_L are the air and water volumetric flow rates respectively and $\rho_{G,STP}$ and ρ_L are the gas and liquid mass densities respectively.

The uncertainty of calculated flow parameters and all other calculated uncertainties were found via the partial differential method. For example, the uncertainty in GLR is as follows in Equation 5.

$$\mathrm{u}(\beta) = \sqrt{\left[\frac{\partial\beta}{\partial\dot{\mathrm{m}}_{\mathrm{G}}}\mathrm{u}(\dot{\mathrm{m}}_{\mathrm{G}})\right]^2 + \left[\frac{\partial\beta}{\partial\dot{\mathrm{m}}_{\mathrm{L}}}\mathrm{u}(\dot{\mathrm{m}}_{\mathrm{L}})\right]^2} = \sqrt{\left[\frac{1}{\dot{\mathrm{m}}_{\mathrm{L}}}\mathrm{u}(\dot{\mathrm{m}}_{\mathrm{G}})\right]^2 + \left[\frac{\dot{\mathrm{m}}_{\mathrm{G}}}{\dot{\mathrm{m}}_{\mathrm{L}}^2}\mathrm{u}(\dot{\mathrm{m}}_{\mathrm{L}})\right]^2} \qquad \text{Eqn. 5}$$

Both air and water inlet pressures were measured with McMaster-Carr digital high-accuracy pressure gauges with a range of 0 to 10 bar and an accuracy of ±1% of full scale (0.1 bar)

3.4.3 Droplet Image Analysis

Droplet size data was collected 60 millimeters downstream of the exit orifices on the centerline of the spray via green diffuse laser shadowgraphy. 60 millimeters was chosen as the distance as it is approximately 30 diameters downstream of the largest tested atomizer exit orifice diameter (CF4 and CF5 D_0=2.341mm) at which point all atomizers should have sprays that are sufficiently atomized, generally noted as the relaxation point of the spray. A Nikon D90 DSLR equipped with a 2x Nikon teleconverter and Infinity DistaMax K2 with CF-4 Objective and 1.66x CF Tube produced a 1 × 0.67mm field of view with 3 image pixels per micron. A Quantel EverGreen Nd:YAG laser provided 145 millijoule 532 nanometer green pulses with an exposure time of <10 nanoseconds and the cameras exposure time limited to obtain only a single image per single laser pulse.

Raw images were processed using ImageJ (Version 1.51K) to identify droplets as small as 3 microns in diameter using a rolling ball background removal tool and intensity threshold technique to distinguish droplets in focus from the background [31] [32]. Droplet areas were measured using the analyze particles function and were converted to diameter assuming a spherical shape. Pre and post-processing image examples are shown in Figure 11.

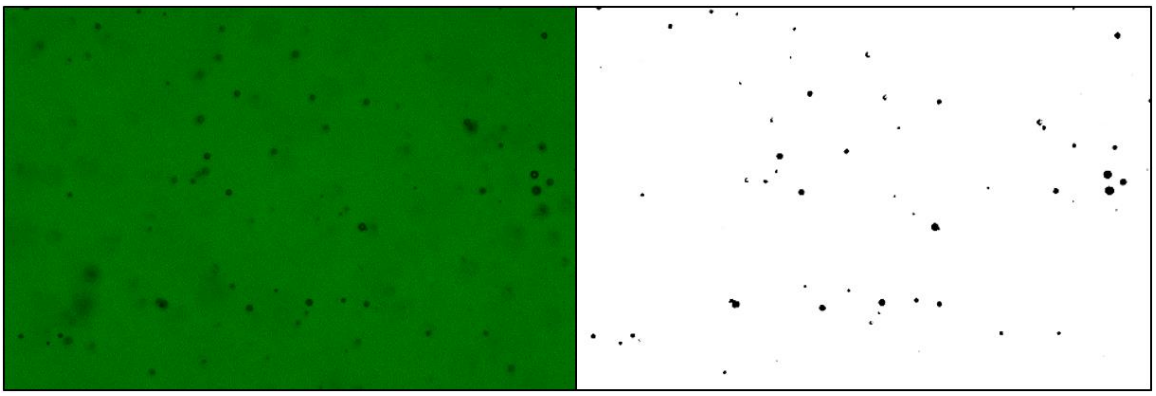

Figure 11. Raw Image (Left) and Processed Image (Right) using ImageJ.

For any given liquid volumetric flow rate and GLR combination, 500-2000 processable, raw images were collected for processing. The total number of droplets counted for a liquid volumetric flow rate and GLR combination ranged from a minimum of 20,000 to well over 100,000 individual droplets. Although the accuracy of SMD was not determined directly, SMD repeatability was ensured by requiring less than 1% variation in SMD over the last 500 identified droplets [27]. Liquid flow rate and GLR combinations that produced sprays with images with an average of 0 to 10 droplets per image with 50% or more having 0 droplets were discarded due to processing difficulties.

Chapter 4 Data Analysis

4.1 Results

4.1.1 Air vs Water Pressure

The measured inlet air and water pressures for each tested counterflow atomizer geometry was found to increase with increasing GLR and water volumetric flow rate. Using atomizer CF3 as a reference, the air and water pressures are plotted in Figure 12. The water pressures are marked with filled diamonds and solid lines while air pressure is marked with unfilled diamonds and dashed lines. It can be seen that the air pressure is greater than the water pressure for the same liquid volumetric flow rate and GLR, which holds true for every atomizer tested in this study. Furthermore, this difference in the air and water pressure was found to be greater for atomizers with greater exit orifice area to air injection annulus area ratios (A_0/A_N).

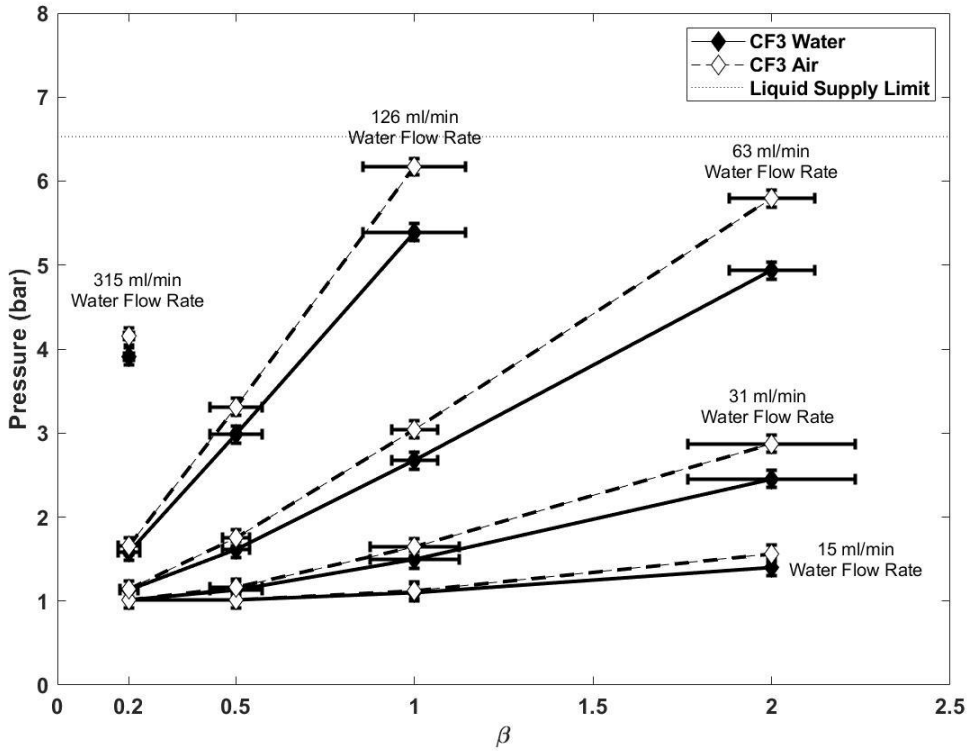

Figure 12. CF3 Air vs Water Pressures ($^{A_0}/_{A_N} = 1.264$). *Water pressures marked with dashed lines and unfilled markers, air pressures marked with solid lines and filled markers. Liquid supply pressure limit of 551 kPa (80 psig)*

4.1.2 Air and Water Pressure vs SMD

In general, SMD was found to decrease with increasing air and water pressures across all 5 tested counterflow atomizer geometries. This relationship is plotted in Figure 13 for air and Figure 14 for water respectively. Geometry CF1 is marked by filled circles; geometry CF2 is marked by unfilled squares; geometry CF3 is

marked by filled diamonds; geometry CF4 is marked by filled stars; and geometry CF5 is marked by unfilled, left-pointing triangles. For continuity and clarity, all 5 counterflow atomizer geometries are represented by the same markers for the remainder of the figures. It can be seen that for a given geometry, a range of SMD values can be found at approximately the same pressures. For example, comparing the SMDs of atomizer CF3 at a liquid pressure of 1.13 bar, a liquid flow rate of 63.1 ml/min at a GLR of 0.2 produced a spray resulting in a centerline SMD of 31.4 microns. At the same pressure, a lower liquid flow rate of 31.5 ml/min at a greater GLR of 0.5 produced a spray resulting in a centerline SMD of 25.9 microns as seen in Table 3.

Table 3. CF3 SMD at a Water Pressure of 1.13 bar

Water Volumetric Flow Rate	GLR	SMD
63.1 ml/min	0.2	31.4 microns
31.5 ml/min	0.5	25.9 microns

It can also be seen that nearly equal SMDs can be achieved for a given geometry at different pressures. For example, atomizer CF3 produced an SMD of 17.3 microns at a liquid pressure of 3.91 bar, a liquid flow rate of 315.5 ml/min, and at a GLR of 0.2. However, atomizer CF3 also produced an SMD of 17.4 microns at a liquid pressure of 1.61 bar, a liquid flow rate of 63.1 ml/min, and at a GLR of 0.5 respectively as seen in Table 4.

Table 4. CF3 Flow Settings for an SMD of Approximately 17 Microns

Liquid Pressure	Water Volumetric Flow Rate	GLR	SMD
3.91 bar	315.5 ml/min	0.2	17.3 microns
1.61 bar	63.1 ml/min	0.5	17.4 microns

Furthermore, comparing geometries it can be seen that the largest SMDs found in this study produced by the atomizers CF3, CF4, and CF5 which had the largest exit orifice diameters.

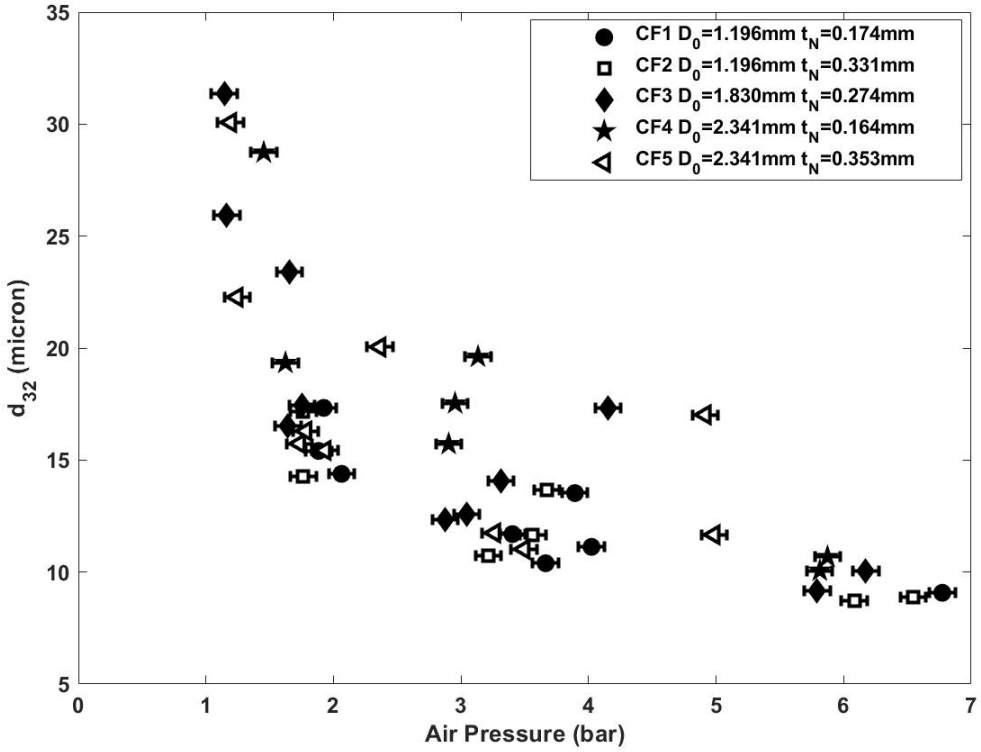

Figure 13. All Geometries – Measured Inlet Air Pressure vs SMD. CF1 (filled circles), CF2 (unfilled squares), CF3 (filled diamonds), CF4 (filled stars), CF5 (unfilled left-pointing triangles)

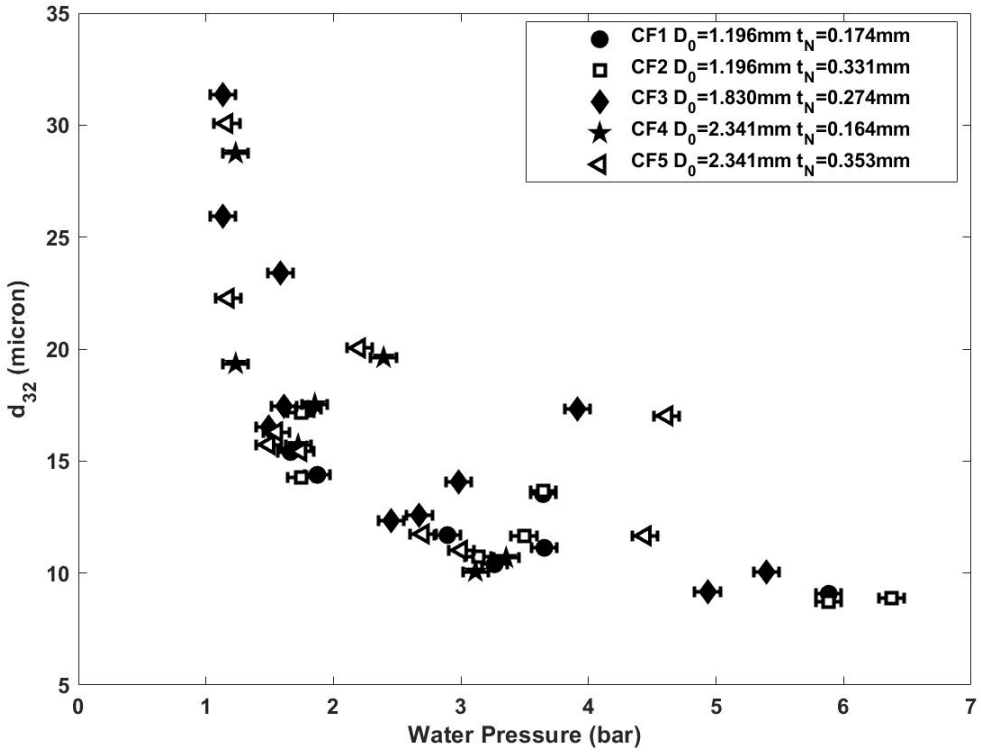

Figure 14. All Geometries – Measured Inlet Water Pressure vs SMD. CF1 (filled circles), CF2 (unfilled squares), CF3 (filled diamonds), CF4 (filled stars), CF5 (unfilled left-pointing triangles)

4.1.3 Effect of Flow Rate and GLR on SMD

Like other methods of twin-fluid atomization, the counterflow atomizers tested in this study showed evidence of diminishing returns on SMD with increasing gas flow rates. All 5 tested counterflow atomizer geometries were plotted as scatter plots of the tested flow settings with their respective calculated SMDs for each setting noted (see figures 36-40 in the appendix for each individual geometry).

Using atomizer CF3 as a reference, the combinations of liquid volumetric flow rates and GLR that yielded a spray with sufficient droplets to collect SMD data is plotted in Figure 15 (Figure 38 in the appendix) with each setting's respective calculated SMD labeled (SMD dimensions in microns). The shape of the plot is due to the pressure limit of the liquid supply instrumentation (reference Figure 12. CF3 Air vs Liquid Pressure). It can be seen that increasing GLR at a constant liquid volumetric flow rate results in a decreasing SMD with diminishing returns. For atomizer CF3, at a liquid volumetric flow rate of 63.1 ml/min (~1.05E-6 m^3/s), increasing the GLR from 0.2 to 0.5 causes an approximate 45% decrease in SMD for a 150% increase in air mass flow rate. Further increasing the GLR from 0.5 to 1.0, a 100% increase in the mass flow rate of air, caused a subsequent decrease in SMD of approximately 28%. Increasing the GLR from 1.0 to 2.0, a 100% increase in the mass flow rate of air, caused a subsequent decrease in SMD approximately 27%.

increasing the liquid volumetric flow rate at a constant GLR, which in effect is increasing both liquid mass flow rate and gas mass flow rate at a constant ratio, also causes a decrease in SMD with diminishing returns. For example, at a fixed GLR of 0.2, doubling the liquid volumetric flow rate from 63.1 ml/min (~1.05E-6 m^3/s) to 126.2 ml/min (~2.1E-6 m^3/s) caused an approximate 25% decrease in SMD. Further increasing the liquid volumetric flow rate from 126.2 ml/min (~2.1E-

6 m^3/s) to 315.5 ml/min (5.26E-6 m^3/s), a 150% increase in flow rate, caused a decrease in SMD of approximately 25% as well.

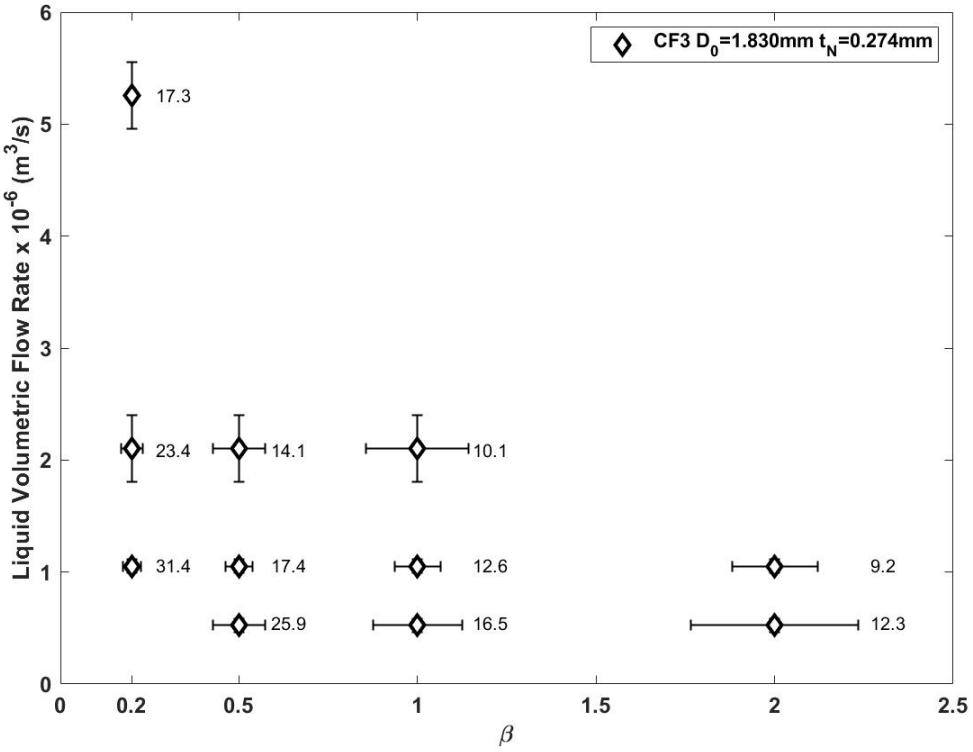

Figure 15. CF3 GLR vs Liquid Volumetric Flow Rate (data labels are SMD in micron)

To isolate the effects of the air and water flow rates independent of one-another, a surface for atomizer CF3 was plotted using linear interpolation between the test points. The air and water volumetric flow rates were converted into air and water mass flow rates respectively which yielded the surface in Figure 16. the yellow to

blue gradient signifies the z-axis SMD values, with yellow being the largest SMDs and blue the smallest (Dark to light gradient in grayscale). It can be seen that with increasing mass flow rate of air the SMD is decreasing with diminishing returns in the form of the decreasing slope in the air mass flow rate – SMD (d_{32}) plane. In contrast, increasing liquid mass flow rate causes a slight increase in SMD, which can be seen in the non-linear increasing slope in the water mass flow rate – SMD (d_{32}) plane.

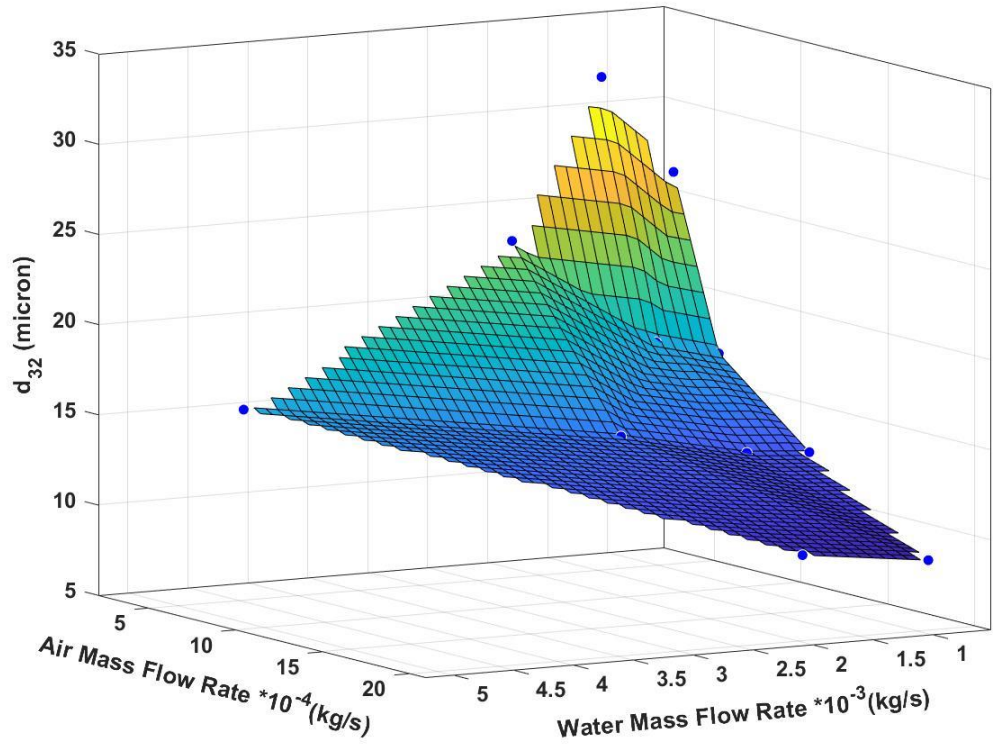

Figure 16. CF3 Air and Water Mass Flow Rates vs SMD. error bars removed for clarity

4.1.4 Effect of Doubling Annulus Thickness, t_N on SMD

The effect of approximately doubling the annulus thickness (t_N) at a constant exit orifice diameter (D_0) on SMD was found to be minimal, with calculated SMD values being within 2 microns between each compared atomizer. Atomizers CF1 and CF2 are plotted in Figure 17 where the SMDs found for CF1 are outlined with solid-lined text boxes and the SMDs for CF2 are outlined with dash-lined text boxes. Similarly, atomizers CF4 and CF5 are plotted in Figure 18 where the SMDs found for CF4 are outlined with solid-lined text boxes and the SMDs for CF5 are outlined with dash-lined text boxes. It can be seen that comparing atomizers CF1 and CF2 at the same flow conditions, SMD values differ by less than 1 micron across all comparable settings. Similarly, comparing atomizers CF4 and CF5 the SMD values differ by less than 2 microns. Additionally, although there are locations for which SMD data was able to be collected for one atomizer and not the other, it is suspected that with a sufficient number of droplets, the SMD values would also be nearly equal.

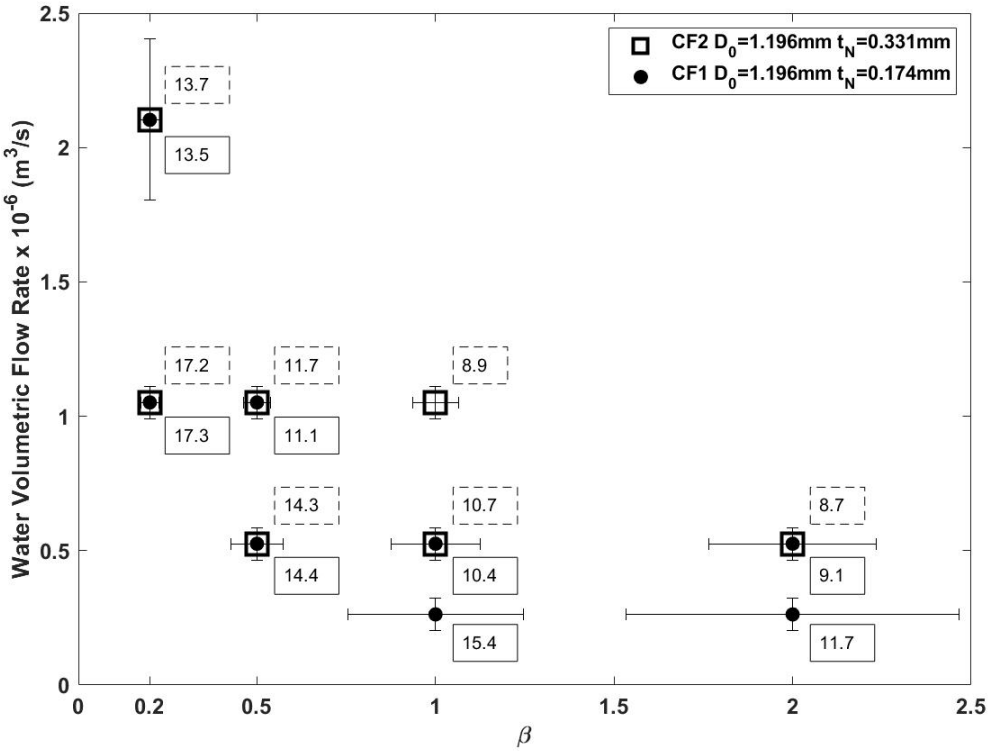

Figure 17. CF1 vs CF2 – GLR vs Liquid Volumetric Flow Rate (SMD in microns). CF1 (filled circles, solid-lined text boxes), CF2 (unfilled squares, solid-lined text boxes)

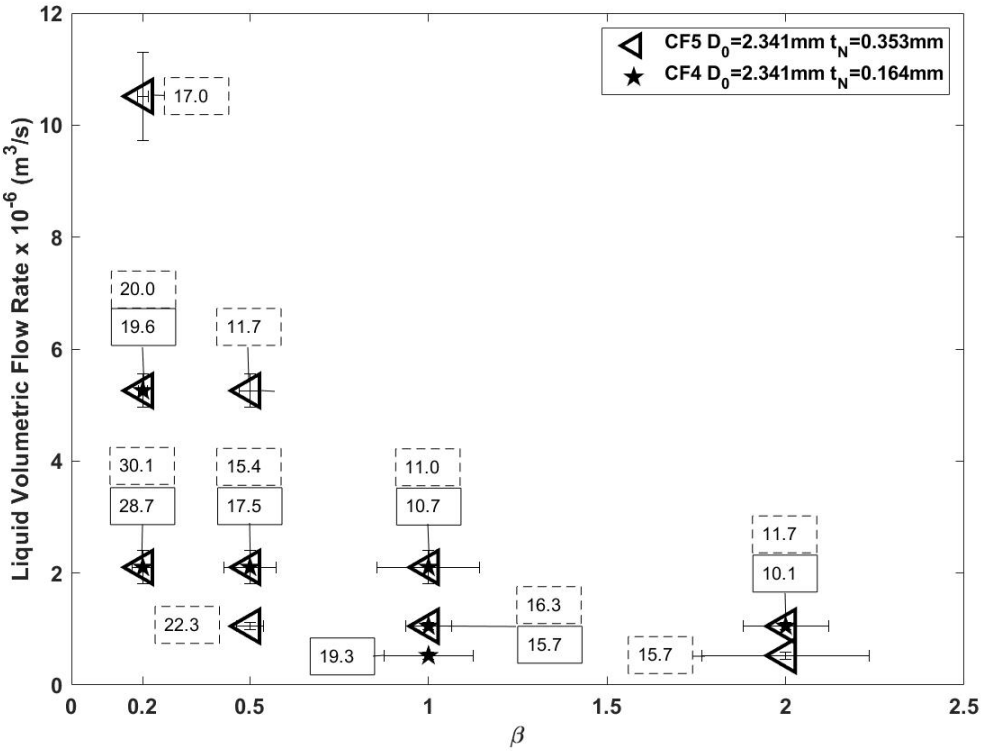

Figure 18. CF4 vs CF5 – GLR vs Liquid Volumetric Flow Rate (SMD in microns). CF4 (filled stars, solid-lined text boxes), CF5 (unfilled left-pointing triangles, solid-lined text boxes)

As with atomizer CF3, surface plots were created by converting the air and water volumetric flow rates to air and water mass flow rates respectively, with atomizers CF1 and CF2 being compared in Figure 19 and atomizers CF4 and CF5 being compared in Figure 20. In both cases, the surfaces created overlap, suggesting that increasing the annulus gap thickness doesn't necessarily change

the interactions in terms of diminishing returns between mass flow rates and the subsequent centerline SMDs produced.

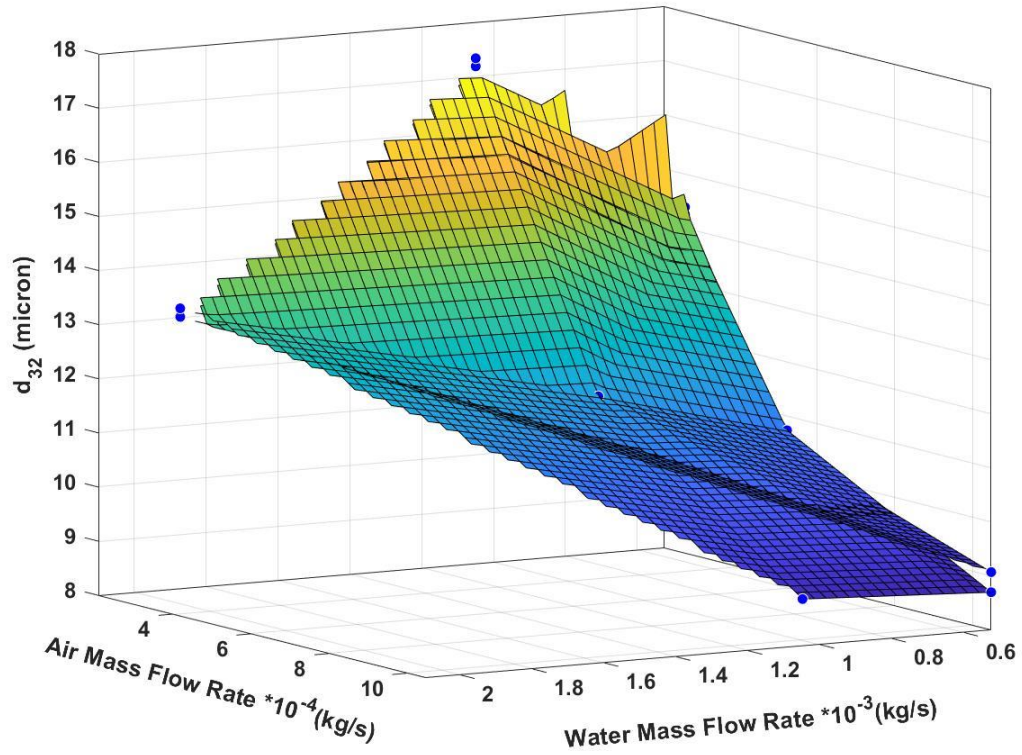

Figure 19. CF1 vs CF2 – Air and Water Mass Flow Rates vs SMD. error bars removed for clarity

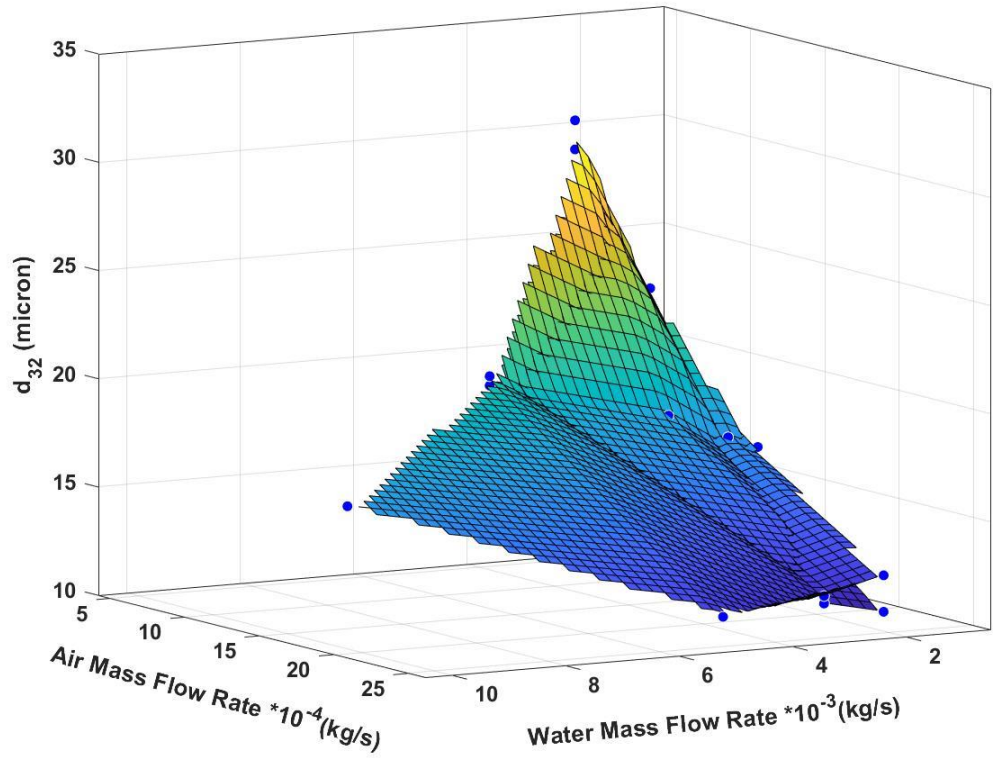

Figure 20. CF4 vs CF5 – Air and Water Mass Flow Rates vs SMD. error bars removed for clarity

4.1.5 Effect of Doubling Exit Diameter, D_0 on SMD

In contrast to doubling annulus thickness (t_N) at a constant exit orifice diameter (D_0), doubling the exit orifice diameter at an approximately constant annulus thickness reveals SMDs dependence on the atomizer exit orifice diameter. Atomizers CF1 and CF4 are plotted in Figure 21 where solid-lined text boxes represent SMDs for CF1 and dash-lined text boxes represent atomizer CF4. Atomizers CF2 and CF5 are plotted in Figure 22 where solid-lined text boxes

represent SMDs for CF2 and dash-lined text boxes represent SMDs for atomizer CF5. Comparing the flow conditions for which both geometries produced a spray in which SMDs were found, the geometry with double the exit orifice diameter produced an SMD that was approximately double the smaller atomizer's as seen in Table 5.

Table 5. Effects of Doubling Exit Diameter on SMD

Atomizer	Water Volumetric Flow Rate (ml/min)	Water Volumetric Flow Rate (m^3/s)	GLR (β)	SMD (micron)
CF1 vs CF4				
CF1	31.5	5.26E-07	1.0	10.4
CF4	31.5	5.26E-07	1.0	19.3
CF1	126.2	2.10E-06	0.2	13.5
CF4	126.2	2.10E-06	0.2	28.7
CF2 vs CF5				
CF2	31.5	5.26E-07	2.0	8.7
CF5	31.5	5.26E-07	2.0	15.7
CF2	63.1	1.05E-06	0.5	11.7
CF5	63.1	1.05E-06	0.5	22.3
CF2	63.1	1.05E-06	1.0	8.9
CF5	63.1	1.05E-06	1.0	16.3
CF2	126.2	2.10E-06	0.2	13.7
CF5	126.2	2.10E-06	0.2	30.1

In Figures 21 and 22, it can be seen that atomizers CF1 and CF2 operated at lower liquid flow rate and GLR combinations than their counterparts CF4 and CF5 with larger exit diameters. That being said, atomizers CF1 and CF2 are

predicted to operate at higher flow rates but data collection was limited by the 551 kPa (80 psig) liquid supply pressure limit.

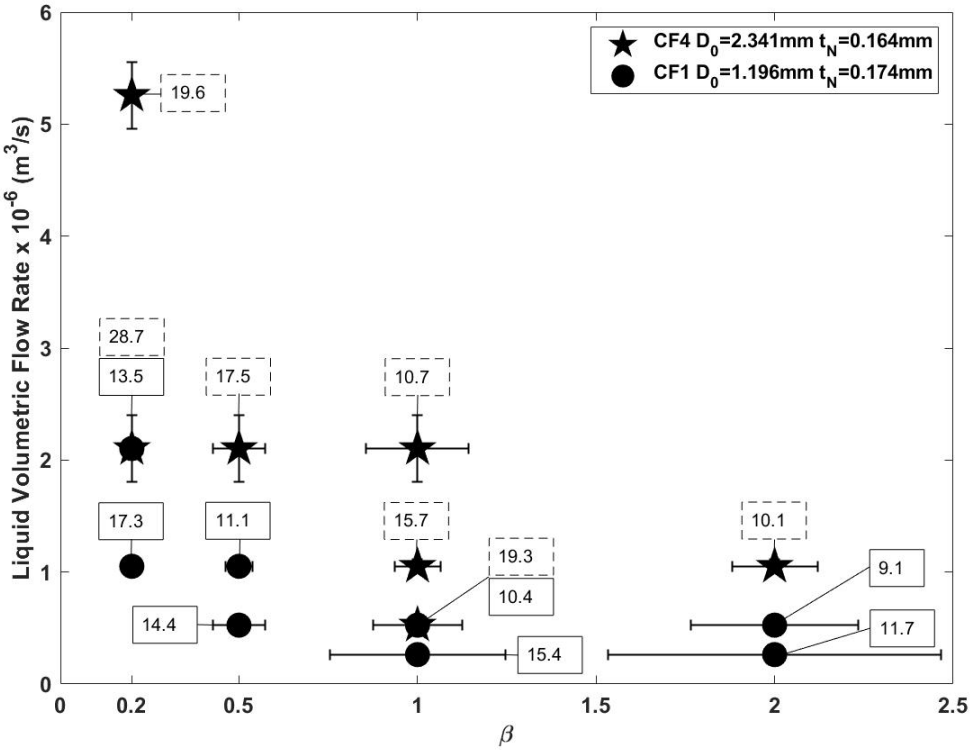

Figure 21. CF1 vs CF4 - GLR vs Liquid Volumetric Flow Rate (SMD in microns). CF1 (filled circles), CF2 (Filled stars)

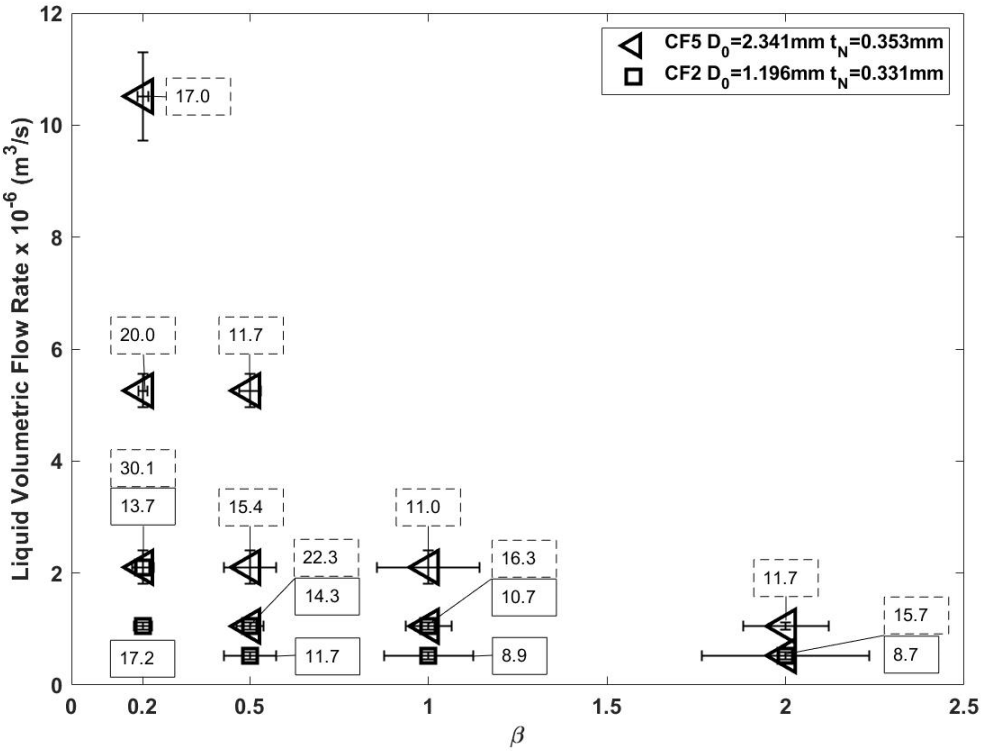

Figure 22. CF2 vs CF5 - GLR vs Liquid Volumetric Flow Rate (SMD in microns). CF2 (unfilled squares), CF5 (unfilled left-pointing triangles)

As with atomizer CF3, surface plots were created by converting the air and water volumetric flow rates to air and water mass flow rates respectively. In Figures 23 and 24, the surface created for the atomizers with larger exit orifice diameters CF4 and CF5 are offset above atomizers CF1 and CF2 but appear to both have the same general shape in which SMD decreases with increasing air mass flow rate with diminishing returns and SMD increases with increasing mass flow rate of water.

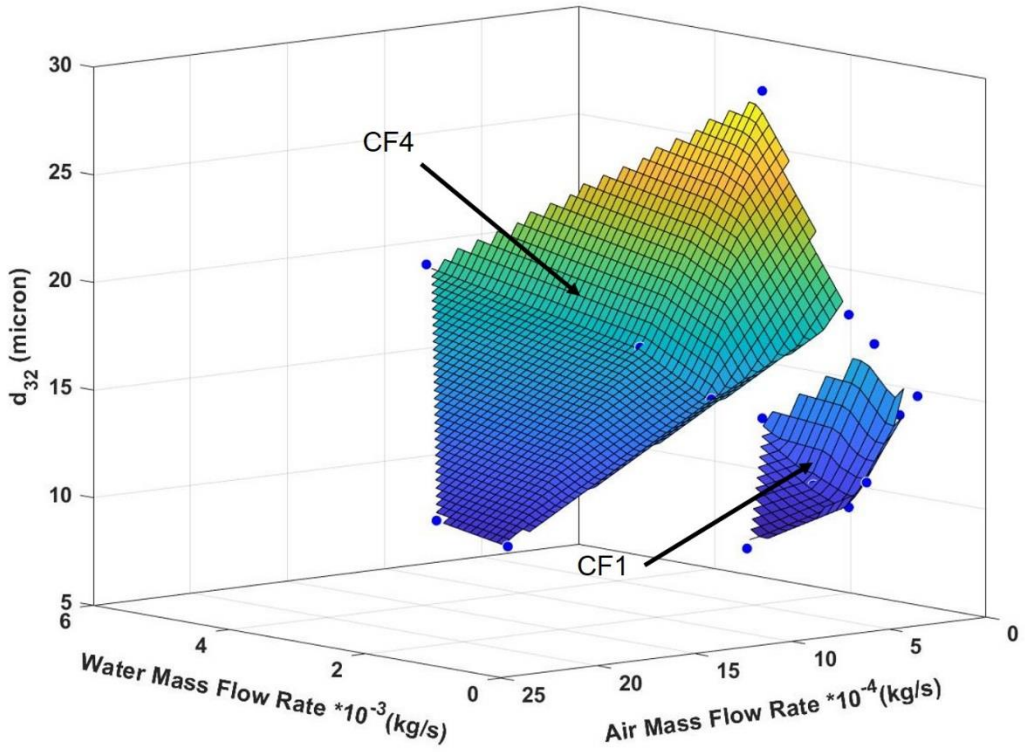

Figure 23. CF1 vs CF4 – Air and Water Mass Flow Rates vs SMD. error bars removed for clarity

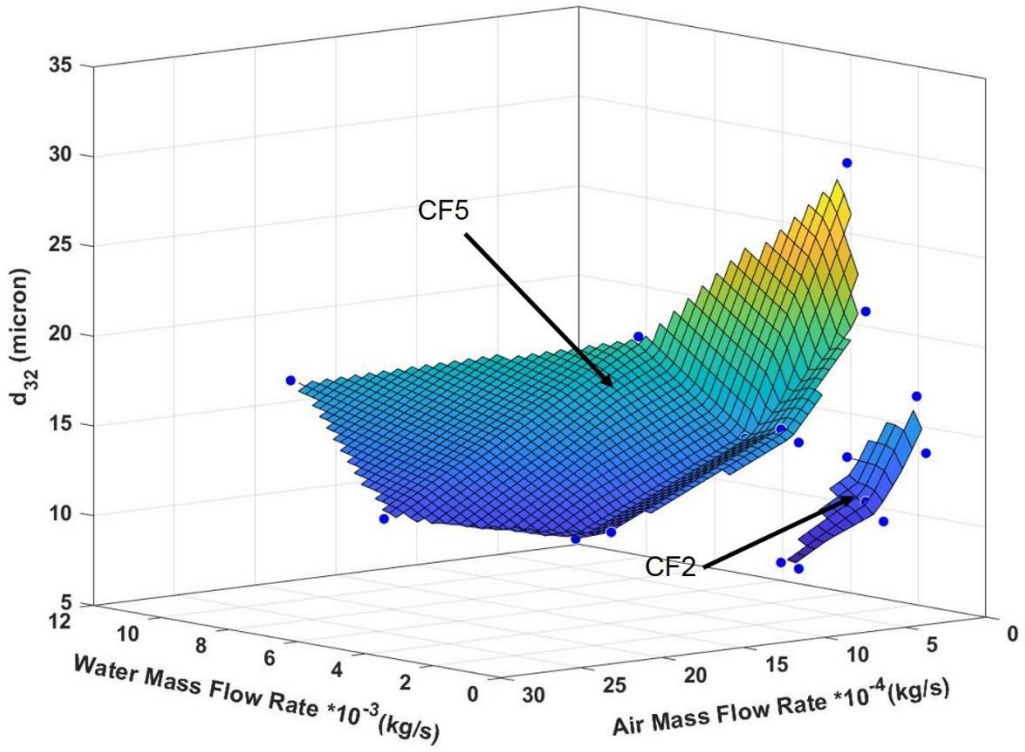

Figure 24. CF2 vs CF5 – Air and Water Mass Flow Rates vs SMD. error bars removed for clarity

4.2 Discussion

4.2.1 Effect of Counterflow Geometry on SMD

Simultaneously plotting the air and water mass flow rates against the SMD of all the tested atomizer geometries reveals a system of roughly parallel surfaces as seen in Figures 25 and 26 in which the surfaces are stacked from top to bottom in order of decreasing exit orifice diameter (CF5 & CF4 → CF3 → CF2 & CF1).

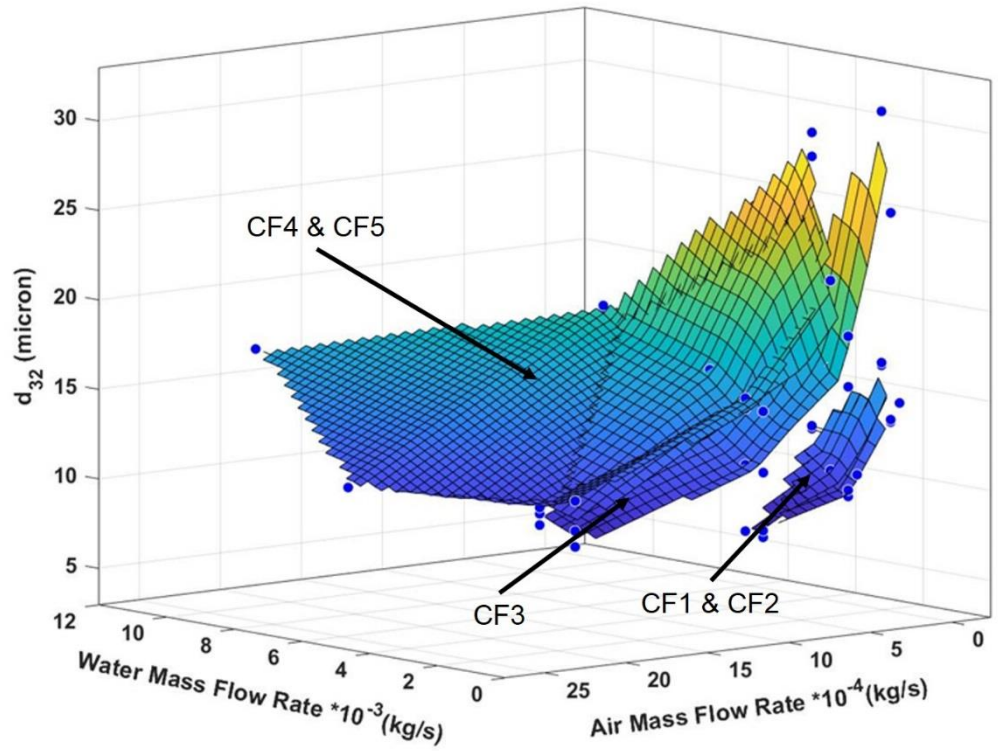

Figure 25. All Geometries – Air and Water Mass Flow Rates vs SMD. error bars removed for clarity

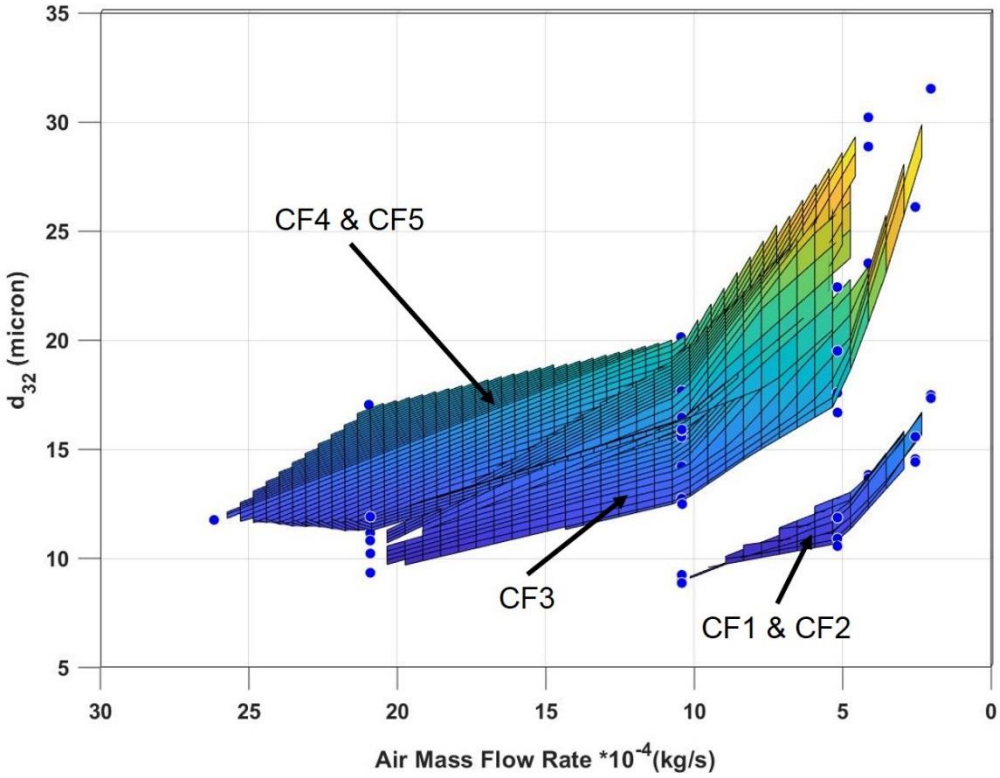

Figure 26. All Geometries – Air and Water Mass Flow Rates vs SMD (Air Mass Flow Rate – SMD plane). error bars removed for clarity

Furthermore, nondimensionalizing SMD by exit orifice diameter yields the surface as seen in Figures 27 and 28. It can be seen that all the surfaces roughly collapse into a single surface which suggests that the centerline SMD produced by counterflow atomizers scale proportionally with exit orifice diameter.

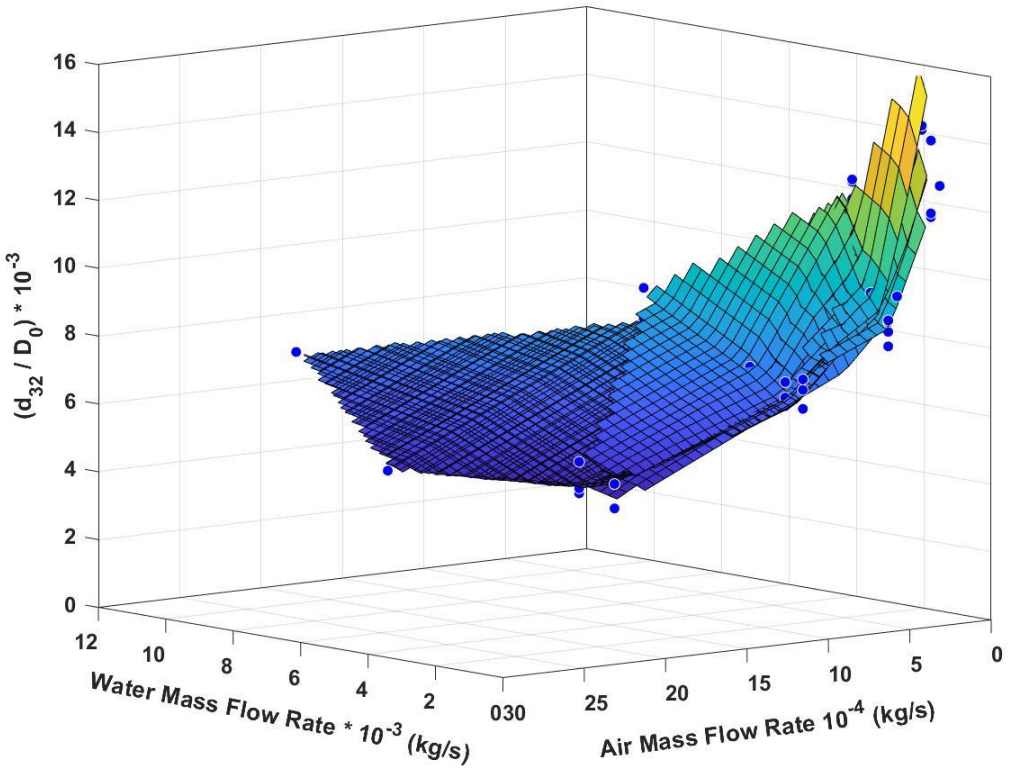

Figure 27. All Geometries, SMD/D_0 – Air and Water Mass Flow Rates vs SMD.

error bars removed for clarity

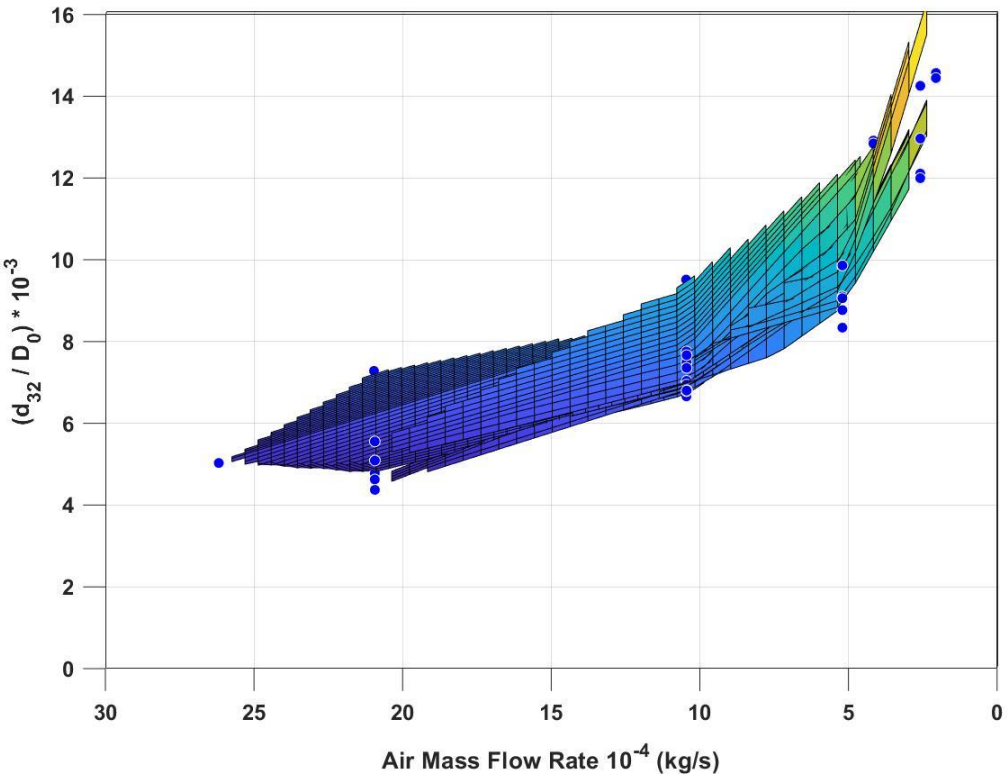

Figure 28. All Geometries, SMD/D_0 – Air and Water Mass Flow Rates vs SMD. error bars removed for clarity

4.2.2 Proposed Counterflow Model

Based on the aforementioned results, the preliminary model for counterflow atomization posed by Johnson in [21] and [27] was modified such that rather than nondimensionalizing SMD by annulus thickness (t_N), it is nondimensionalized by exit orifice diameter (D_0), where the densities are calculated at atmospheric pressure. Plotting this modified model is shown in Figure 29. It can be seen that

vertical lines form which, from left to right are 2.0, 1.0, 0.5, and 0.2 GLR respectively for the atomizers tested in this study.

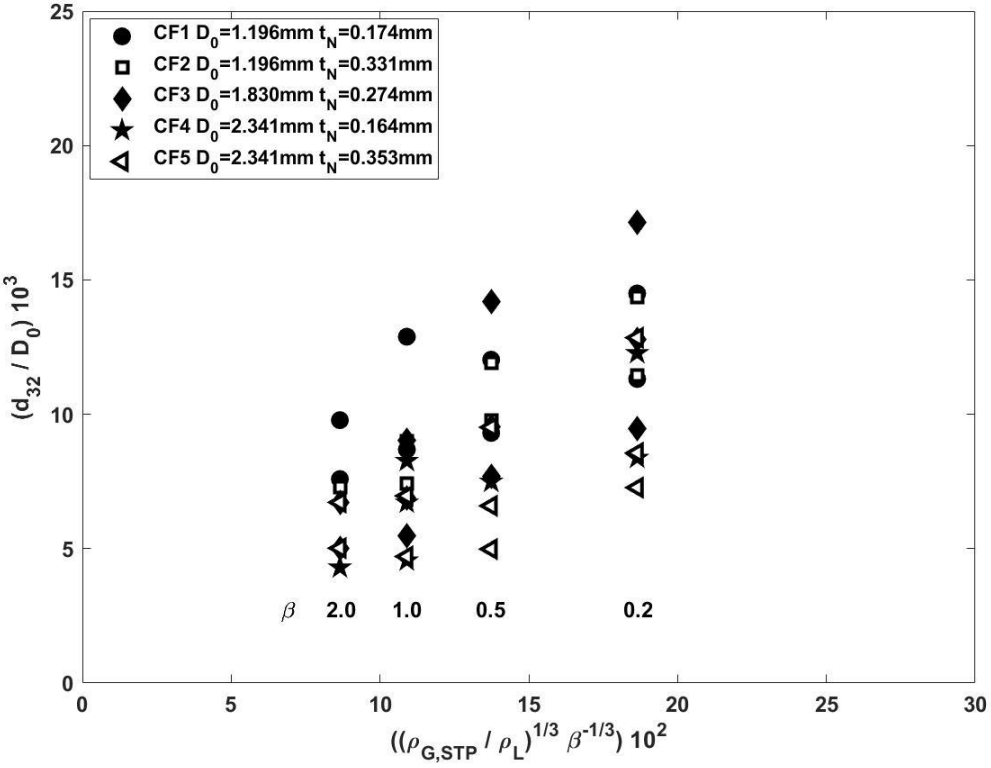

Figure 29. Modified Counterflow Model. CF1 (filled circles), CF2 (unfilled squares), CF3 (filled diamonds), CF4 (filled stars), CF5 (unfilled left-pointing triangles)

4.2.3 Effect of Counterflow Geometry on RSF

Previous examinations of counterflow atomization have revealed a positive linear correlation of RSF with SMD that was not found in this study [21] [22]. The RSF

is plotted against the SMD for all tested counterflow atomizer geometries in Figure 30.

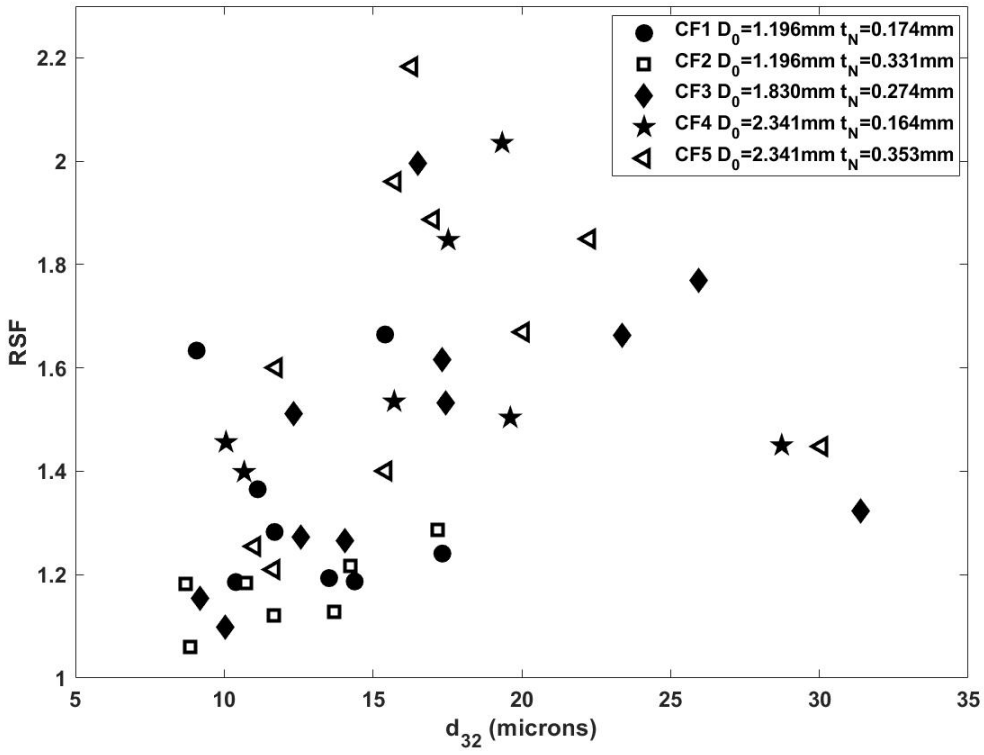

Figure 30. SMD vs RSF. CF1 (filled circles), CF2 (unfilled squares), CF3 (filled diamonds), CF4 (filled stars), CF5 (unfilled left-pointing triangles)

Plotting the SMD against the individual components of RSF ($D_{0.1}$, $D_{0.5}$, $D_{0.9}$), reveals the variance in RSF was caused by the variation in the 90th volume-weighted droplet diameter distribution.

The 10th volume-weighted droplet diameter distribution, $D_{0.1}$ is plotted against SMD in Figure 31. It can be seen that it displays a positive, linear correlation between $D_{0.1}$ and SMD with an R^2 of 0.924 and has 2 outliers present from atomizers CF1 and CF3.

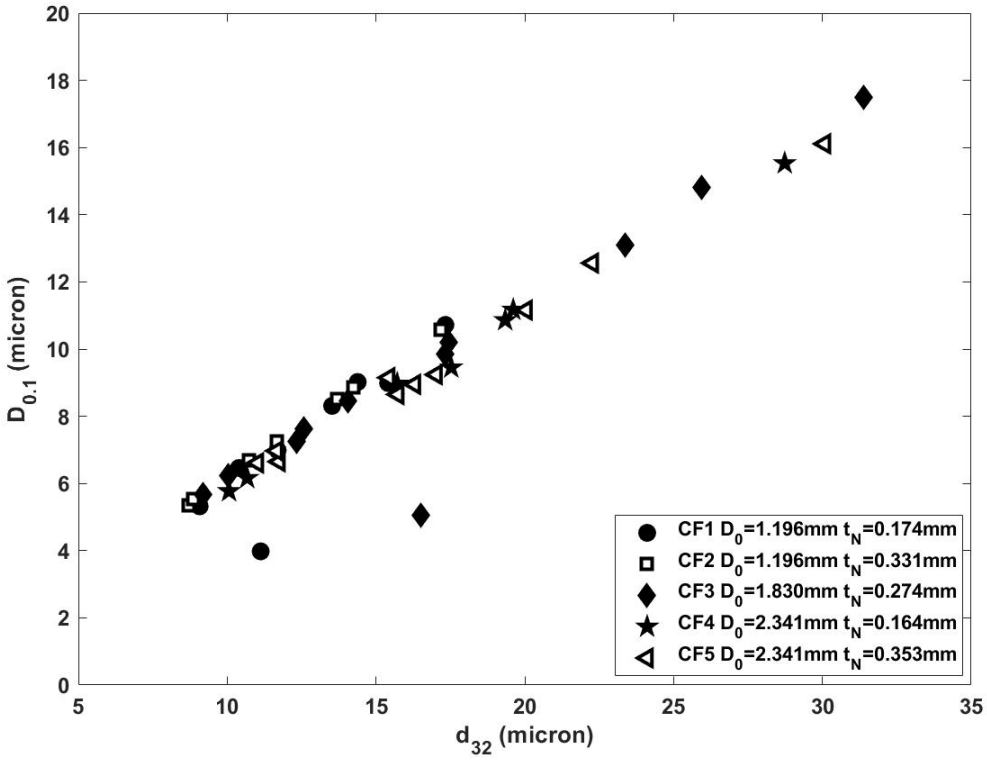

Figure 31. SMD vs $D_{0.1}$. CF1 (filled circles), CF2 (unfilled squares), CF3 (filled diamonds), CF4 (filled stars), CF5 (unfilled left-pointing triangles)

The 50th volume-weighted droplet diameter distribution, $D_{0.5}$ (also referred to as MMD) is plotted against SMD in Figure 32. Like $D_{0.1}$, plotting $D_{0.5}$ against SMD also reveals a positive-linear correlation with an R^2 of 0.992.

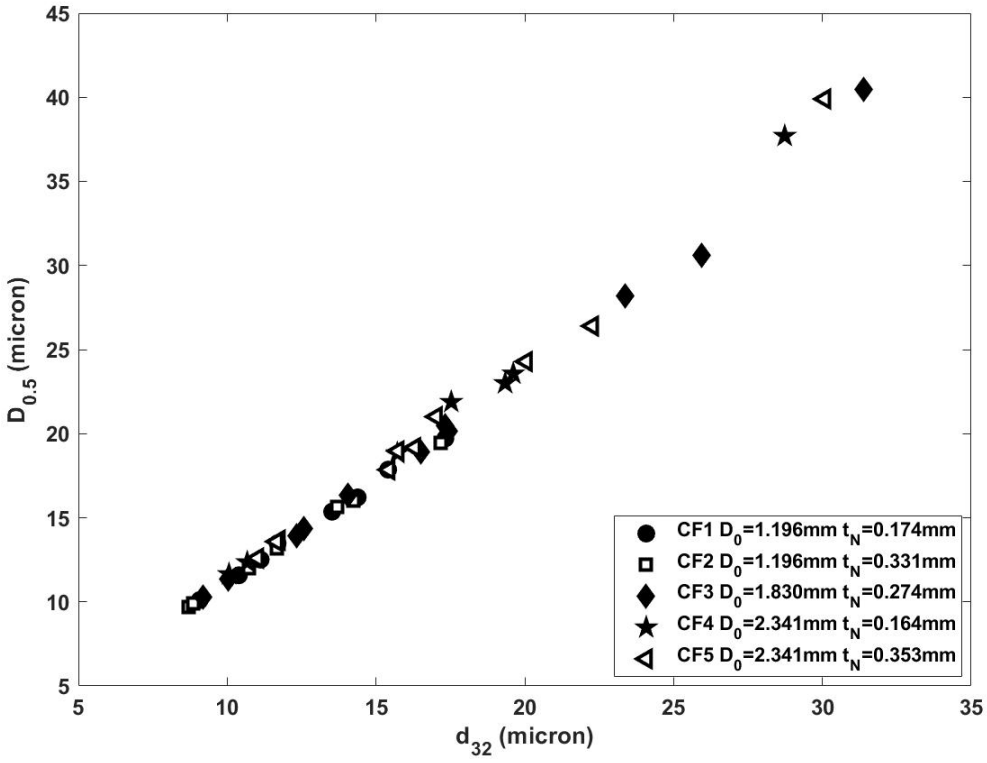

Figure 32. SMD vs $D_{0.5}$. CF1 (filled circles), CF2 (unfilled squares), CF3 (filled diamonds), CF4 (filled stars), CF5 (unfilled left-pointing triangles)

The 90th volume-weighted droplet diameter distribution, $D_{0.9}$ is plotted against SMD in Figure 33. As mentioned, $D_{0.9}$ was found to have a larger variance and a weaker positive correlation with SMD with an R^2 of 0.921. However, this is not unexpected as some of the flow settings tested in this study are on the outside limits of where atomization occurs for counterflow atomizers and as such, provide less narrow drop size distributions with larger outlying droplets.

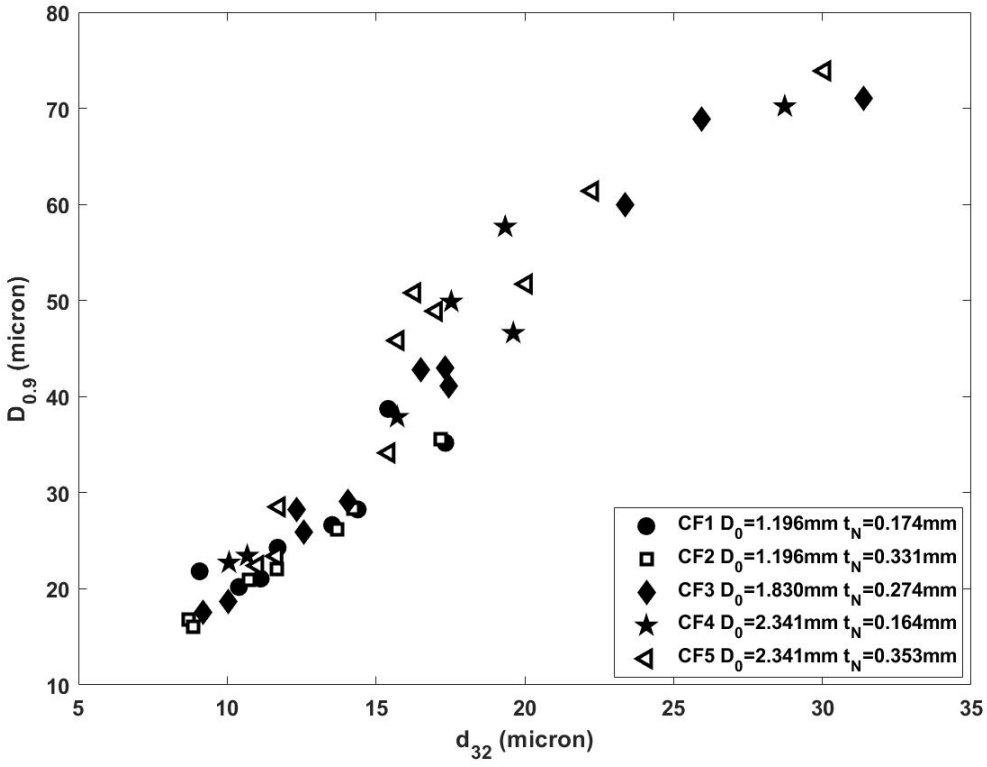

Figure 33. SMD vs $D_{0.9}$. CF1 (filled circles), CF2 (unfilled squares), CF3 (filled diamonds), CF4 (filled stars), CF5 (unfilled left-pointing triangles)

Chapter 5 Conclusion

The centerline SMD produced by counterflow atomization 60 millimeters downstream of the exit orifice appears to be minimally affected by the annulus thickness t_N and instead, proportional to the exit orifice diameter D_0 for the geometries and flow settings tested.

The RSF found in this study varies more widely than previous counterflow literature and doesn't display a positive correlation with SMD. Rather, the individual components of RSF $D_{0.1}$ and $D_{0.5}$ both show the positive linear correlation as seen in previous counterflow studies while $D_{0.9}$ suffers from larger drop sizes and more variation due to the ranges of flow settings tested in this study.

Bibliography

[1] E. Michaelides, C. Crowe and J. Schwarzkopf, Multiphase Flow handbook, CRC Press, 2017.

[2] A. Lefebvre and V. Mcdonell, Atomization and Sprays 2nd Edition, CRC Press, 2017.

[3] C. Crowe, J. Schwarzkopf, M. Sommerfeld and Y. Tsuji, Multiphase Flows with Droplets and Particles, CRC Press, 2012.

[4] N. Asgriz, Handbook of Atomization and SPrays Theory and Applications, Springer, 2011.

[5] H. Merkus, Particle Size Measurements Fundamentals, Practice, Quality, Springer, 2009.

[6] H. Liu, Science and Engineering of Droplets Fundamentals and Applications, Detroit: Noyes Publications, 2000.

[7] K. K. Uoong, K. J. Youn and L. S. Yong, "Determination of In-Focus Criteria and Depth of Field in Image Processing of Spray Particles," *Atomization and Sprays,* vol. 11, pp. 317-333, 2001.

[8] J. Kashdan, J. Shrimpton and A. Whybrew, "Two-Phase Flow Characterization by Automated Digital Image Analysis. Part 1: Fundamental Principles and Calibration of the Technique," *Particle and Particle Systems Characterization,* vol. 20, no. 6, pp. 387-397, 2003.

[9] K. Kim and S. Kim, "Drop Sizing and Depth-of-Field Correction in TV Imaging," *Atomization and Sprays,* vol. 4, pp. 65-78, 1994.

[10] R. Murugan and P. Kolhe, "Experimental Investigation into Flow Blurring Atomization," *Experimental Thermal and Fluid Science,* vol. 120, 2021.

[11] M. Khan, H. Gadgil and S. Kumar, "Influence of Liquid Properties on Atomization Characteristics of Flow-Blurring Injector at Ultra-Low Flow Rates," *Energy,* vol. 171, pp. 1-13, 2019.

[12] B. Fisher, M. Weismiller, S. Tuttle and K. Hinnant, "Effects of Fluid Properties on Spray Characteristics of a Flow-Blurring Atomizer," *Journal of Engineering for Gas Turbines and Power,* vol. 140, no. 4, 2018.

[13] B. Simmons and A. Agrawal, "Flow Blurring Atomization for Low-Emission Combustion of Liquid Biofuels," *Combustion Science and Technology,* vol. 184, no. 5, pp. 660-675, 2012.

[14] A. M. Gañán-Calvo, "Enhanced Liquid Atomization: From Flow-Focusing to Flow-Blurring," *Applied Physics Letters,* vol. 86, no. 21, pp. 1-3, 2005.

[15] A. Garbaly and T. Shepard, "Impact of Bubble Size on Flow Response to Transient Pressure Drop Through Converging Nozzle," in *ASME 2020 Fluids Engineering Division Summer Meeting*, 2020.

[16] T. Shepard and A. Garbaly, "Experimental Investigation of Choked Flow Conditions for Bubbly Flow," in *ASME-JSME-KSME 2019 8th Joint Fluids Engineering Conference*, 2019.

[17] N. Mikvik and B. Knizat, "On the Spray Pulsations of the Effervescent Atomizers," in *EFM 2017 EPJ Web of Conferences*, 2017.

[18] D. Konstantinov, R. Marsh, P. Bowen and A. Crayford, "Effervescent Atomization for Industrial Energy-Technology Review.," *Atomization and Sprays,* vol. 20, no. 6, pp. 525-552, 2010.

[19] M. Lörcher, F. Schmidt and D. Mewes, "Effervescent Atomization of Liquids," *Atomization and Sprays,* vol. 15, no. 2, pp. 145-068, 2005.

[20] S. Sovani, P. Sojka and A. Lefebvre, "Effervescent Atomization," *Progress in Energy and Combustion Science,* vol. 27, no. 4, pp. 483-521, 2001.

[21] E. Johnson, V. Srinivasan, P. Strykowski and A. Hoxie, "Role of Density in Gas-Assist Counterflow Atomization," in *ILASS-Americas 30th Annual Conference on Liquid Atomization and Spray Systems*, 2019.

[22] A. Hoxie, E. Johnson, V. Srinivasan and P. Strykowski, "Characterization of a Novel Energy Efficient Atomizer Employing Countercurrent Shear," in *ICLASS 2018, 14th Triennial International Conference on Liquid Atomization and Spray Systems*, 2018.

[23] H. Zhang, A. Hoxie, R. Rangarajan, P. Strykowski and V. Srinivasan, "Atomization of HIgh Viscosity Liquids Using a Two-Fluid Counterflow Nozzle: Experiments and Modeling," in *GT2020 ASME Turbo Expo 2020*, 2020.

[24] V. Sividas, M. Heitor and R. Fernandas, "A Functional Correlation for the Primary Breakup Processes of Liquid Sheets Emerging from Air-Assist Atomizers," *Journal of Fluids Engineering, Transactions of the ASME,* vol. 129, no. 2, pp. 188-193, 2007.

[25] Y. Levy, V. Shermaum, V. Ovcharenko and V. Nadvani , "Study of Two Miniature Air-Assist Atomizers with Radial and Axial Air Swirlers," in *GT2006 ASME Turbo Expo: Power for Land, Sea and Air*, 2006.

[26] D. Miller and A. H. Lefebvre, "The Development of an Air Blast Atomizer for Gas Turbine Application," College of Aeronatutics Cranfield, 1966.

[27] E. Johnson, "Thesis: The influence of Injection Gas Molar Mass on Counterflow Atomizer Performance," University of Minnesota, 2019.

[28] T. C. Roesler and A. H. Lefebvre, "Studies on Aerated-Liquid Atomization," *International Journal of Turbo and Jet Engines,* vol. 6, no. 3-4, 1989.

[29] J. Li, A. H. Lefebvre and J. R. Rollbuhler, "Effervescent Atomizers for Small Gas Turbines," in *American Society of Mechanical Engineers 94-GT-495*, 1994.

[30] D. J. Forliti, B. A. Tang and P. J. Strykowski, "An experimental investigation of planar countercurrent turbulent shear layers," *Journal of Fluid Mechanics,* vol. 530, pp. 241-264, 2005.

[31] T. D. Fansler and S. E. Parrish, "Spray measurement technology: a review," *Measurement Science and Technology,* vol. 26, 2015.

[32] S. Y. Lee, B. S. Park and I. G. Kim, "Gray Level Factors used in Image Processing of Two-Dimensional Drop Images," *Atomization and Sprays,* vol. 1, pp. 389-400, 1991.

[33] A. H. Lefebvre, "Twin-Fluid Atomization: Factors Influencing Mean Drop Size," *Atomization and Sprays,* vol. 2, pp. 101-119, 1992.

Appendix

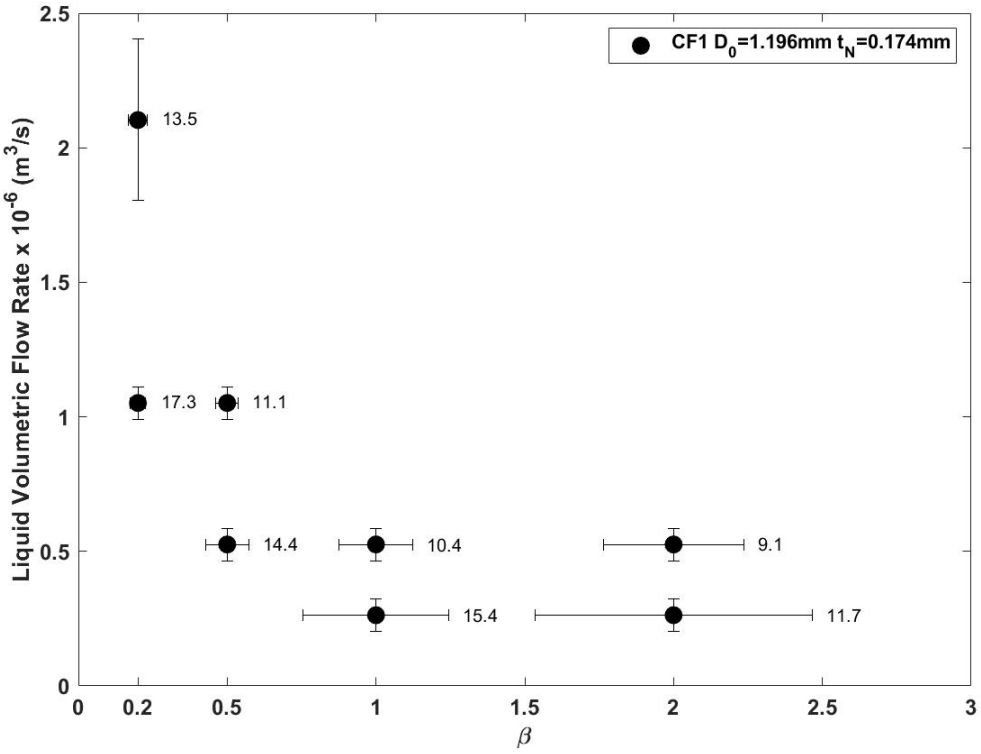

Figure 34. CF1 Liquid Volumetric Flow Rate vs GLR (SMD in microns)

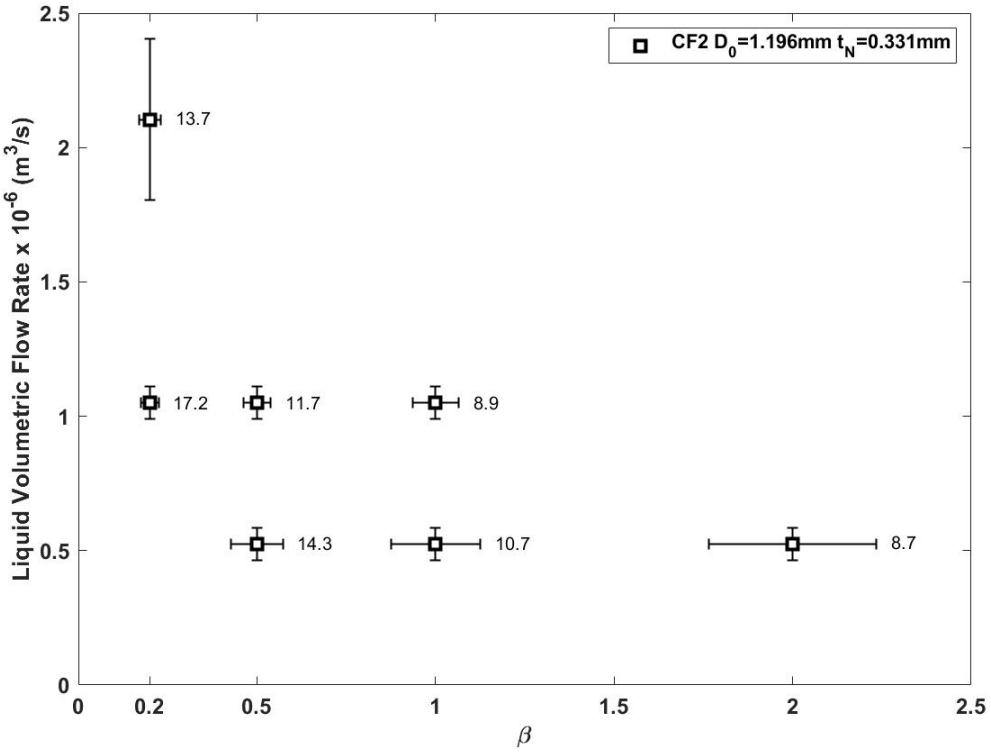

Figure 35. CF2 Liquid Volumetric Flow Rate vs GLR (SMD in microns)

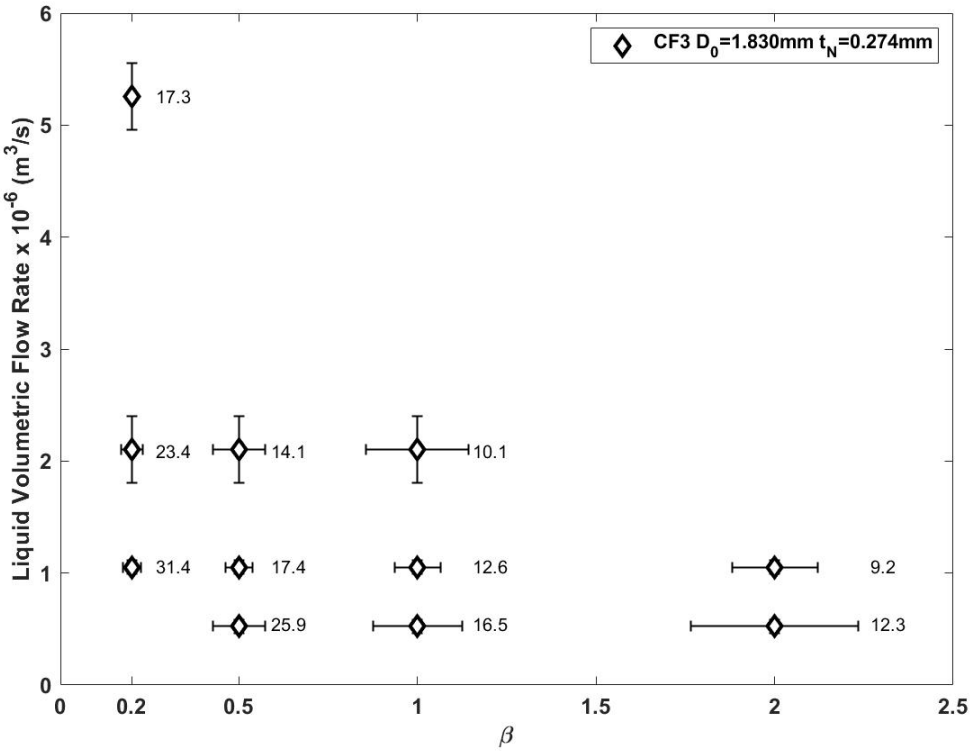

Figure 36. CF3 Liquid Volumetric Flow Rate vs GLR (SMD in microns)

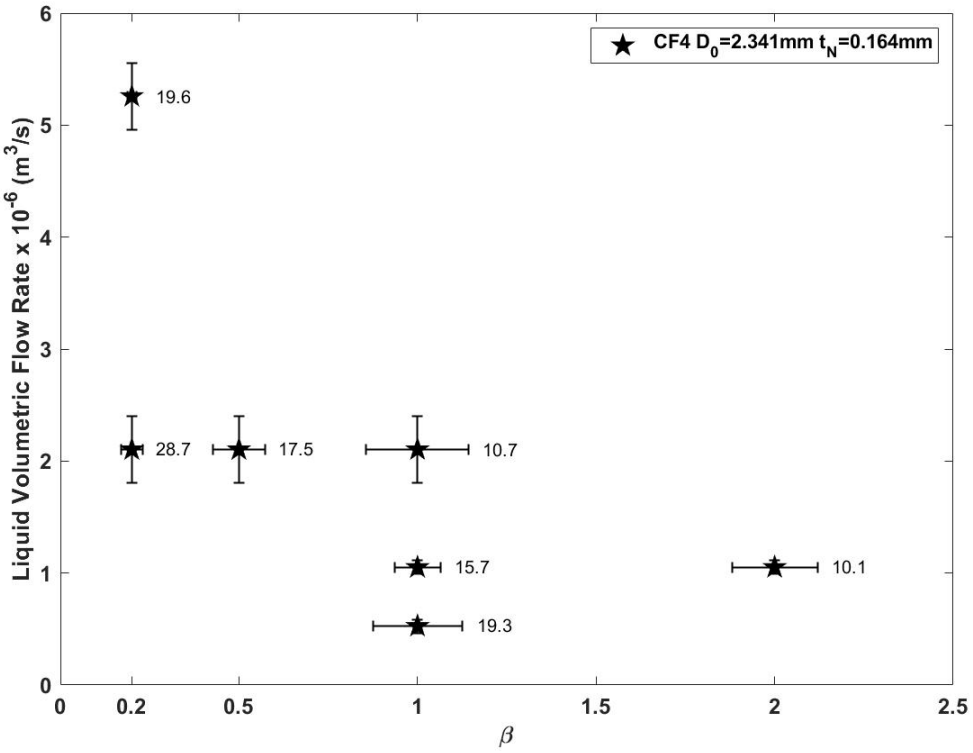

Figure 37. CF4 Liquid Volumetric Flow Rate vs GLR (SMD in microns)

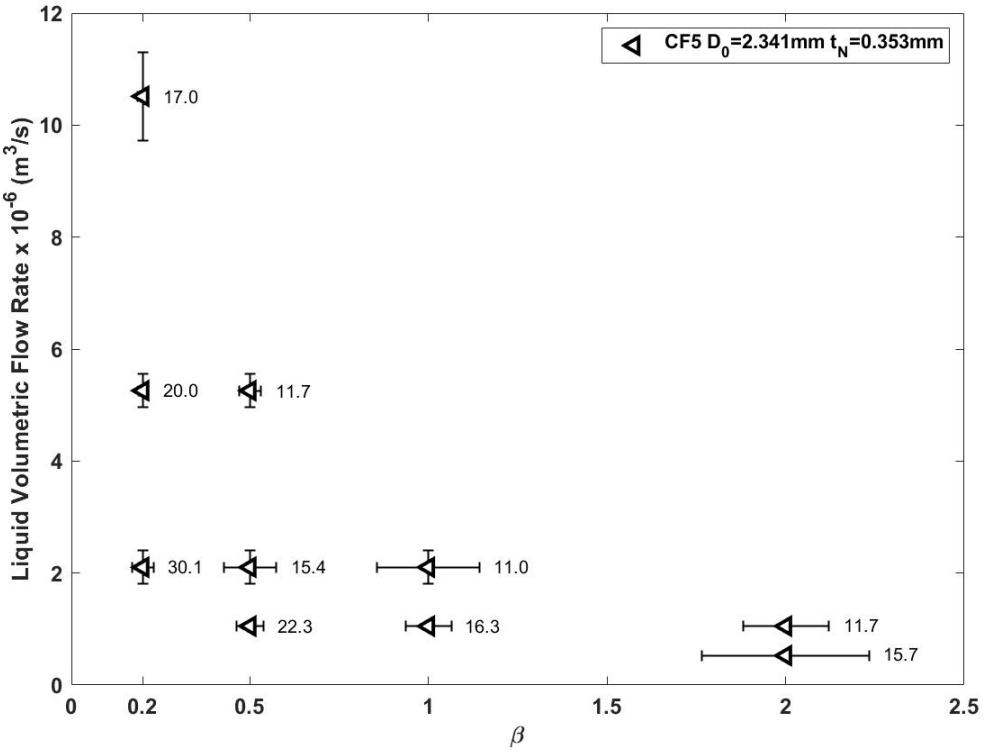

Figure 38. CF5 Liquid Volumetric Flow Rate vs GLR (SMD in microns)